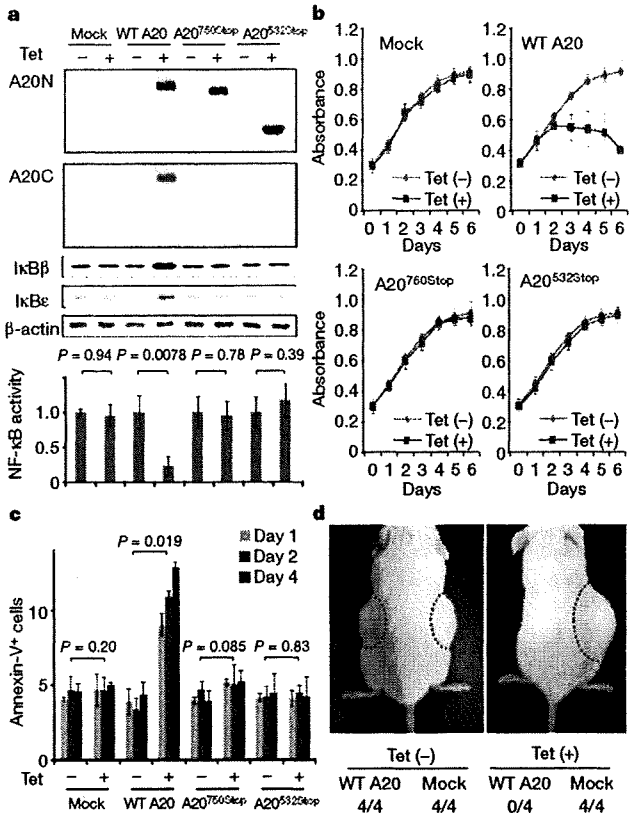

Figure 2 | Effects of wild-type and mutant A20 re-expressed in a lymphoma cell line that lacks the normal *A20* gene. a, Western blot analyses of wild-type (WT) and mutant ($A20^{532Stop}$ and $A20^{750Stop}$) A20, as well as IκBβ and IκBε, in KM-H2 cells, in the presence or absence of tetracycline treatment (top panels). A20N and A20C are polyclonal antisera raised against N-terminal and C-terminal A20 peptides, respectively. β-actin blots are provided as a control. NF-κB activities are expressed as mean absorbance ± s.d. ($n = 6$) in luciferase assays (bottom panel). **b,** Proliferation of KM-H2 cells stably transduced with plasmids for mock and *Tet*-inducible wild-type A20, $A20^{532Stop}$ and $A20^{750Stop}$ was measured using a cell counting kit in the presence (red lines) or absence (blue lines) of tetracycline. Mean absorbance ± s.d. ($n = 5$) is plotted. **c,** The fractions of Annexin-V-positive KM-H2 cells transduced with various *Tet*-inducible A20 constructs were measured by flow cytometry after tetracycline treatment and the mean values (±s.d., $n = 3$) are plotted. **d,** *In vivo* tumorigenicity was assayed by inoculating 7×10^6 KM-H2 cells transduced with mock or *Tet*-inducible wild-type A20 in NOG mice, with (right panel) or without (left panel) tetracycline administration.

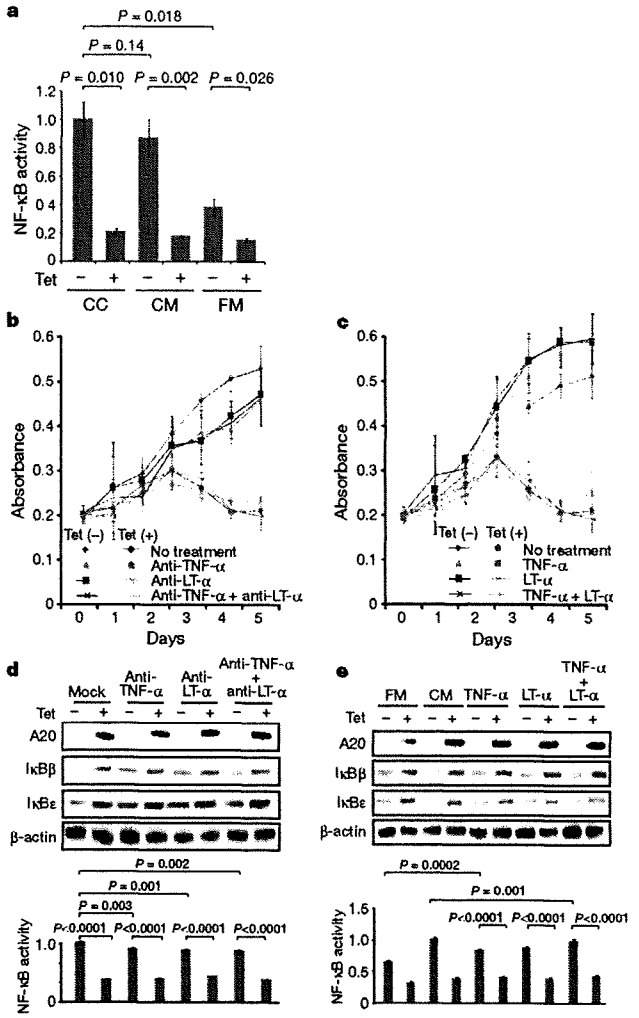

Figure 3 | Tumour suppressor role of A20 under external stimuli. a, NF-κB activity in KM-H2 cells was measured 30 min after cells were inoculated into fresh medium (FM) or KM-H2-conditioned medium (CM) obtained from the 48-h culture of KM-H2, and was compared with the activity after 48 h continuous culture of KM-H2 (CC). A20 was induced 12 h before inoculation in Tet (+) groups. **b, c,** Effects of neutralizing antibodies against TNF-α and lymphotoxin-α (LTα) (**b**) and of recombinant TNF-α and LT-α added to the culture (**c**) on cell growth were evaluated in the presence (Tet (+)) or absence (Tet (−)) of A20 induction. Cell numbers were measured using a cell counting kit and are plotted as their mean absorbance ± s.d. ($n = 6$). **d, e,** Effects of the neutralizing antibodies (**d**) and the recombinant cytokines added to the culture (**e**) on NF-κB activities and the levels of IκBβ and IκBε after 48 h culture with (Tet (+)) or without (Tet (−)) tetracycline treatment. NF-κB activities are expressed as mean absorbance ± s.d. ($n = 6$) in luciferase assays.

negative feedback mechanism in the regulation of NF-κB signalling pathways upon a variety of stimuli, aberrant activation of NF-κB will be a logical consequence of A20 inactivation. However, there is also the possibility that the aberrant NF-κB activity of A20-inactivated lymphoma cells is derived from upstream stimuli, which may be from the cellular environment. In this context, it is intriguing that MALT lymphoma usually arises at the site of chronic inflammation caused by infection or autoimmune disorders and may show spontaneous regression after eradication of infectious organisms[28]; furthermore, Hodgkin's lymphoma frequently shows deregulated cytokine production from Reed–Sternberg cells and/or surrounding reactive cells[29]. Detailed characterization of the NF-κB pathway regulated by A20 in both normal and neoplastic B lymphocytes will promote our understanding of the precise roles of A20 inactivation in the pathogenesis of these lymphoma types. Our finding underscores the importance of genome-wide approaches in the identification of genetic targets in human cancers.

METHODS SUMMARY

Genomic DNA from 238 patients with non-Hodgkin's lymphoma and three Hodgkin's-lymphoma-derived cell lines was analysed using GeneChip SNP genotyping microarrays (Affymetrix). This study was approved by the ethics boards of the University of Tokyo, National Cancer Institute Hospital, Okayama University, and the Cancer Institute of the Japanese Foundation of Cancer Research. After appropriate normalization of mean array intensities, signal ratios between tumours and anonymous normal references were calculated in an allele-specific manner, and allele-specific copy numbers were inferred from the observed signal ratios based on the hidden Markov model using CNAG/AsCNAR software (http://www.genome.umin.jp). *A20* mutations were examined by directly sequencing genomic DNA using a set of primers (Supplementary Table 6). Full-length cDNAs of wild-type and mutant *A20* were introduced into a

lentivirus vector, pLenti4/TO/V5-DEST (Invitrogen), with a *Tet*-inducible promoter. Viral stocks were prepared by transfecting the vector plasmids into 293FT cells (Invitrogen) using the calcium phosphate method and then infected to the KM-H2 cell line. Proliferation of KM-H2 cells was measured using a Cell Counting Kit (Dojindo). Western blot analyses and luciferase assays were performed as previously described. NF-κB activity was measured by luciferase assays in KM-H2 cells stably transduced with a reporter plasmid having an NF-κB response element, pGL4.32 (Promega). Apoptosis of KM-H2 upon A20 induction was evaluated by counting Annexin-V-positive cells by flow cytometry. For *in vivo* tumorigenicity assays, 7×10^6 KM-H2 cells were transduced with the *Tet*-inducible *A20* gene and those with a mock vector were inoculated on the contralateral sides in eight NOG mice[19] and examined for their tumour formation with ($n = 4$) or without ($n = 4$) tetracycline administration. Full copy number data of the 238 lymphoma samples will be accessible from the Gene Expression Omnibus (GEO, http://ncbi.nlm.nih.gov/geo/) with the accession number GSE12906.

Full Methods and any associated references are available in the online version of the paper at www.nature.com/nature.

Received 17 September 2008; accepted 3 March 2009.
Published online 3 May 2009.

1. Dixit, V. M. *et al.* Tumor necrosis factor-α induction of novel gene products in human endothelial cells including a macrophage-specific chemotaxin. *J. Biol. Chem.* **265**, 2973–2978 (1990).
2. Song, H. Y., Rothe, M. & Goeddel, D. V. The tumor necrosis factor-inducible zinc finger protein A20 interacts with TRAF1/TRAF2 and inhibits NF-κB activation. *Proc. Natl Acad. Sci. USA* **93**, 6721–6725 (1996).
3. Lee, E. G. *et al.* Failure to regulate TNF-induced NF-κB and cell death responses in A20-deficient mice. *Science* **289**, 2350–2354 (2000).
4. Boone, D. L. *et al.* The ubiquitin-modifying enzyme A20 is required for termination of Toll-like receptor responses. *Nature Immunol.* **5**, 1052–1060 (2004).
5. Wang, Y. Y., Li, L., Han, K. J., Zhai, Z. & Shu, H. B. A20 is a potent inhibitor of TLR3- and Sendai virus-induced activation of NF-κB and ISRE and IFN-β promoter. *FEBS Lett.* **576**, 86–90 (2004).
6. Wertz, I. E. *et al.* De-ubiquitination and ubiquitin ligase domains of A20 downregulate NF-κB signalling. *Nature* **430**, 694–699 (2004).
7. Heyninck, K. & Beyaert, R. A20 inhibits NF-κB activation by dual ubiquitin-editing functions. *Trends Biochem. Sci.* **30**, 1–4 (2005).
8. Graham, R. R. *et al.* Genetic variants near *TNFAIP3* on 6q23 are associated with systemic lupus erythematosus. *Nature Genet.* **40**, 1059–1061 (2008).
9. Musone, S. L. *et al.* Multiple polymorphisms in the *TNFAIP3* region are independently associated with systemic lupus erythematosus. *Nature Genet.* **40**, 1062–1064 (2008).
10. Jaffe, E. S., Harris, N. L., Stein, H. & Vardiman, J. W. *World Health Organization Classification of Tumours. Pathology and Genetics of Tumours of Hematopoietic and Lymphoid Tissues* (IARC Press, 2001).
11. Klein, U. & Dalla-Favera, R. Germinal centres: role in B-cell physiology and malignancy. *Nature Rev. Immunol.* **8**, 22–33 (2008).
12. Nannya, Y. *et al.* A robust algorithm for copy number detection using high-density oligonucleotide single nucleotide polymorphism genotyping arrays. *Cancer Res.* **65**, 6071–6079 (2005).
13. Yamamoto, G. *et al.* Highly sensitive method for genomewide detection of allelic composition in nonpaired, primary tumor specimens by use of affymetrix single-nucleotide-polymorphism genotyping microarrays. *Am. J. Hum. Genet.* **81**, 114–126 (2007).
14. Jost, P. J. & Ruland, J. Aberrant NF-κB signaling in lymphoma: mechanisms, consequences, and therapeutic implications. *Blood* **109**, 2700–2707 (2007).
15. Durkop, H., Hirsch, B., Hahn, C., Foss, H. D. & Stein, H. Differential expression and function of A20 and TRAF1 in Hodgkin lymphoma and anaplastic large cell lymphoma and their induction by CD30 stimulation. *J. Pathol.* **200**, 229–239 (2003).
16. Honma, K. *et al. TNFAIP3* is the target gene of chromosome band 6q23.3-q24.1 loss in ocular adnexal marginal zone B cell lymphoma. *Genes Chromosom. Cancer* **47**, 1–7 (2008).
17. Sarma, V. *et al.* Activation of the B-cell surface receptor CD40 induces A20, a novel zinc finger protein that inhibits apoptosis. *J. Biol. Chem.* **270**, 12343–12346 (1995).
18. Fries, K. L., Miller, W. E. & Raab-Traub, N. The A20 protein interacts with the Epstein-Barr virus latent membrane protein 1 (LMP1) and alters the LMP1/TRAF1/TRADD complex. *Virology* **264**, 159–166 (1999).
19. Hiramatsu, H. *et al.* Complete reconstitution of human lymphocytes from cord blood $CD34^+$ cells using the NOD/SCID/γ^{null} mice model. *Blood* **102**, 873–880 (2003).
20. Hsu, P. L. & Hsu, S. M. Production of tumor necrosis factor-α and lymphotoxin by cells of Hodgkin's neoplastic cell lines HDLM-1 and KM-H2. *Am. J. Pathol.* **135**, 735–745 (1989).
21. Dierlamm, J. *et al.* The apoptosis inhibitor gene *API2* and a novel 18q gene, *MLT*, are recurrently rearranged in the t(11;18)(q21;q21) associated with mucosa-associated lymphoid tissue lymphomas. *Blood* **93**, 3601–3609 (1999).
22. Willis, T. G. *et al.* Bcl10 is involved in t(1;14)(p22;q32) of MALT B cell lymphoma and mutated in multiple tumor types. *Cell* **96**, 35–45 (1999).
23. Joos, S. *et al.* Classical Hodgkin lymphoma is characterized by recurrent copy number gains of the short arm of chromosome 2. *Blood* **99**, 1381–1387 (2002).
24. Martin-Subero, J. I. *et al.* Recurrent involvement of the *REL* and *BCL11A* loci in classical Hodgkin lymphoma. *Blood* **99**, 1474–1477 (2002).
25. Lenz, G. *et al.* Oncogenic *CARD11* mutations in human diffuse large B cell lymphoma. *Science* **319**, 1676–1679 (2008).
26. Deacon, E. M. *et al.* Epstein-Barr virus and Hodgkin's disease: transcriptional analysis of virus latency in the malignant cells. *J. Exp. Med.* **177**, 339–349 (1993).
27. Yin, M. J. *et al.* HTLV-I Tax protein binds to MEKK1 to stimulate IκB kinase activity and NF-κB activation. *Cell* **93**, 875–884 (1998).
28. Isaacson, P. G. & Du, M. Q. MALT lymphoma: from morphology to molecules. *Nature Rev. Cancer* **4**, 644–653 (2004).
29. Skinnider, B. F. & Mak, T. W. The role of cytokines in classical Hodgkin lymphoma. *Blood* **99**, 4283–4297 (2002).

Supplementary Information is linked to the online version of the paper at www.nature.com/nature.

Acknowledgements This work was supported by the Core Research for Evolutional Science and Technology, Japan Science and Technology Agency, by the 21st century centre of excellence program 'Study on diseases caused by environment/genome interactions', and by Grant-in-Aids from the Ministry of Education, Culture, Sports, Science and Technology of Japan and from the Ministry of Health, Labor and Welfare of Japan for the 3rd-term Comprehensive 10-year Strategy for Cancer Control. We also thank Y. Ogino, E. Matsui and M. Matsumura for their technical assistance.

Author Contributions M.Ka., K.N. and M.S. performed microarray experiments and subsequent data analyses. M.Ka., Y.C., K.Ta., J.T., J.N., M.I., A.T. and Y.K. performed mutation analysis of *A20*. M.Ka., S.Mu., M.S., Y.C. and Y.Ak. conducted functional assays of mutant A20. Y.S., K.Ta., Y.As., H.M., M.Ku., S.Mo., S.C., Y.K., K.To. and Y.I. prepared tumour specimens. I.K., K.O., A.N., H.N. and T.N. conducted *in vivo* tumorigenicity experiments in NOG/SCID mice. T.I., Y.H., T.Y., Y.K. and S.O. designed overall studies, and S.O. wrote the manuscript. All authors discussed the results and commented on the manuscript.

Author Information The copy number data as well as the raw microarray data will be accessible from the GEO (http://ncbi.nlm.nih.gov/geo/) with the accession number GSE12906. Reprints and permissions information is available at www.nature.com/reprints. Correspondence and requests for materials should be addressed to S.O. (sogawa-tky@umin.ac.jp) or Y.K. (ykkobaya@ncc.go.jp).

METHODS

Specimens. Primary tumour specimens were obtained from patients who were diagnosed with DLBCL, follicular lymphoma, MCL, MALT lymphoma, or classical Hodgkin's lymphoma. In total, 238 primary lymphoma specimens listed in Supplementary Table 1 were subjected to SNP array analysis. Three Hodgkin's-lymphoma-derived cell lines (KM-H2, HDLM2, L540) were obtained from Hayashibara Biochemical Laboratories, Inc., Fujisaki Cell Center and were also analysed by SNP array analysis.

Microarray analysis. High-molecular-mass DNA was isolated from tumour specimens and subjected to SNP array analysis using GeneChip Mapping 50K and/or 250K arrays (Affymetrix). The scanned array images were processed with Gene Chip Operation software (GCOS), followed by SNP calls using GTYPE. Genome-wide copy number measurements and LOH detection were performed using CNAG/AsCNAR software[12,13].

Mutation analysis. Mutations in the *A20* gene were examined in 265 samples of B-lineage lymphoma, including 62 DLBCLs, 52 follicular lymphomas, 87 MALTs, 37 MCLs and 3 Hodgkin's-lymphoma-derived cell lines and 24 primary Hodgkin's lymphoma samples, by direct sequencing using an ABI PRISM 3130xl Genetic Analyser (Applied Biosystems). To analyse primary Hodgkin's lymphoma samples in which CD30-positive tumour cells (Reed–Sternberg cells) account for only a fraction of the specimen, 150 Reed–Sternberg cells were collected for each 10 μm slice of a formalin-fixed block immunostained for CD30 by laser-capture microdissection (ASLMD6000, Leica), followed by genomic DNA extraction using QIAamp DNA Micro kit (Qiagen). The primer sets used in this study are listed in Supplementary Table 6.

Functional analysis of wild-type and mutant A20. Full-length cDNA for wild-type *A20* was isolated from total RNA extracted from an acute myeloid leukaemia-derived cell line, CTS, and subcloned into a lentivirus vector (pLenti4/TO/V5-DEST, Invitrogen). cDNAs for mutant A20 were generated by PCR amplification using mutagenic primers (Supplementary Table 6), and introduced into the same lentivirus vector. Forty-eight hours after transfection of each plasmid into 293FT cells using the calcium phosphate method, lentivirus stocks were obtained from ultrafiltration using Amicon Ultra (Millipore), and used to infect KM-H2 cells to generate stable transfectants of mock, wild-type and mutant A20. Each KM-H2 derivative cell line was further transduced stably with a reporter plasmid (pGL4.32, Promega) containing a luciferase gene under an NF-κB-responsive element by electroporation using Nucleofector reagents (Amaxa).

Assays for cell proliferation and NF-κB activity. Proliferation of the KM-H2 derivative cell lines was assayed in triplicate using a Cell Counting Kit (Dojindo). The mean absorption of five independent assays was plotted with s.d. for each derivative line. Two independent KM-H2-derived cell lines were used for each experiment. The NF-κB activity in KM-H2 derivatives for A20 mutants was evaluated by luciferase assays using a PiccaGene Luciferase Assay Kit (TOYO B-Net Co.). Each assay was performed in triplicate and the mean absorption of five independent experiments was plotted with s.d.

Western blot analyses. Polyclonal anti-sera against N-terminal (anti-A20N) and C-terminal (anti-A20C) A20 peptides were generated by immunizing rabbits with these peptides (LSNMRKAVKIRERTPEDIC for anti-A20N and CFQFKQMYG for anti-A20C, respectively). Total cell lysates from KM-H2 cells were separated on 7.5% polyacrylamide gel and subjected to western blot analysis using antibodies to A20 (anti-A20N and anti-A20C), IκBα (sc-847), IκBβ (sc-945), IκBγ (sc-7155) and actin (sc-8432) (Santa Cruz Biotechnology).

Functional analyses of wild-type and mutant A20. Each KM-H2 derivative cell line stably transduced with various *Tet*-inducible A20 constructs was cultured in serum-free medium in the presence or absence of A20 induction using 1 μg ml^{-1} of tetracycline, and cell number was counted every day. 1×10^6 cells of each KM-H2 derivative cell line were analysed for their intracellular levels of IκBβ and IκBε and for NF-κB activities by western blot analyses and luciferase assays, respectively, 12 h after the beginning of cell culture. Effects of human recombinant TNF-α and lymphotoxin-α (210-TA and 211-TB, respectively, R&D Systems) on the NF-κB pathway and cell proliferation were evaluated by adding both cytokines into 10 ml of serum-free cell culture at a concentration of 200 pg ml^{-1}. For cell proliferation assays, culture medium was half replaced every 12 h to minimize the side-effects of autocrine cytokines. Intracellular levels of IκBβ, IκBε and NF-κB were examined 12 h after the beginning of the cell culture. To evaluate the effect of neutralizing TNF-α and lymphotoxin-α, 1×10^6 of KM-H2 cells transduced with both *Tet*-inducible A20 and the NF-κB-luciferase reporter were pre-cultured in serum-free media for 36 h, and thereafter neutralizing antibodies against TNF-α (MAB210, R&D Systems) and/or lymphotoxin-α (AF-211-NA, R&D Systems) were added to the media at a concentration of 200 pg ml^{-1}. After the extended culture during 12 h with or without 1 μg ml^{-1} tetracycline, the intracellular levels of IκBβ and IκBε and NF-κB activities were examined by western blot analysis and luciferase assays, respectively. To examine the effects of A20 re-expression on apoptosis, 1×10^6 KM-H2 cells were cultured for 4 days in 10 ml medium with or without *Tet* induction. After staining with phycoerythrin-conjugated anti-Annexin-V (ID556422, Becton Dickinson), Annexin-V-positive cells were counted by flow cytometry at the indicated times.

***In vivo* tumorigenicity assays.** KM-H2 cells transduced with a mock or *Tet*-inducible wild-type *A20* gene were inoculated into NOG mice and their tumorigenicity was examined for 5 weeks with or without tetracycline administration. Injections of 7×10^6 cells of each KM-H2 cell line were administered to two opposite sites in four mice. Tetracycline was administered in drinking water at a concentration of 200 μg ml^{-1}.

ELISA. Concentrations of TNF-α, lymphotoxin-α, IL-1, IL-2, IL-4, IL-6, IL-12, IL-18 and TGF-β in the culture medium were measured after 48 h using ELISA. For those cytokines detectable after 48-h culture (TNFα, LTα, and IL-6), their time course was examined further using the Quantikine ELISA kit (R&D Systems).

Statistical analysis. Significance of the difference in NF-κB activity between two given groups was evaluated using a paired *t*-test, in which the data from each independent luciferase assay were paired to calculate test statistics. To evaluate the effect of A20 re-expression in KM-H2 cells on apoptosis, the difference in the fractions of Annexin-V-positive cells between Tet (+) and Tet (−) groups was also tested by a paired *t*-test for assays, in which the data from the assays performed on the same day were paired.

Histological and immunophenotypic changes in 59 cases of B-cell non-Hodgkin's lymphoma after rituximab therapy

Akiko Miyagi Maeshima,[1,4] Hirokazu Taniguchi,[1] Junko Nomoto,[2] Dai Maruyama,[2] Sung-Won Kim,[2] Takashi Watanabe,[2] Yukio Kobayashi,[2] Kensei Tobinai[2] and Yoshihiro Matsuno[3]

[1]Clinical Laboratory; [2]Hematology and Stem Cell Transplantation Divisions, National Cancer Center Hospital, Tokyo; [3]Department of Surgical Pathology, Hokkaido University Hospital, Sapporo, Japan

(Received June 30, 2008/Revised September 4, 2008/Accepted September 12, 2008/Online publication November 25, 2008)

Rituximab is a chimeric monoclonal antibody that recognizes the CD20 antigen. It has been used to treat B-cell non-Hodgkin lymphoma (B-NHL), but recently rituximab resistance has been a cause for concern. We examined histological and immunohistochemical changes in 59 patients with B-NHL after rituximab therapy. The patients comprised 32 men and 27 women with a median age of 59 years. Pre-rituximab specimens comprised 34 follicular lymphomas (FL), 11 diffuse large B-cell lymphomas (DLBCL), 10 mantle cell lymphomas, two marginal zone B-cell lymphomas (MZBCL), and two chronic lymphocytic leukemias (CLL). CD20 expression in lymphoma cells was evaluated by immunohistochemistry or flow cytometry. Post-rituximab materials were taken a median of 6 months (4 days to 59 months) after rituximab therapy. Sixteen cases (27%) showed loss of CD20 expression with four histological patterns: pattern 1, no remarkable histological change (FL, 5; DLBCL, 3; and CLL, 2); pattern 2, proliferation of plasmacytoid cells (FL, 2; DLBCL, 1; and MZBCL, 1); pattern 3, transformation to classical Hodgkin's lymphoma (FL, 1); and pattern 4, transformation to anaplastic large cell lymphoma-like undifferentiated lymphoma (FL, 1). Loss of CD20 was unrelated to the interval of biopsies, treatment regimen, clinical response, and frequency of rituximab administration. Loss of CD20 within 1 month of rituximab therapy (3/14, 21%) and regain of CD20 (2/7, 29%) were not frequent. CD20-positive relapse with transformation occurred most frequently in cases of early relapse. In conclusion, B-NHL showed various histological and immunophenotypic changes after rituximab therapy, including not only CD20 loss but also proliferation of plasmacytoid cells or transformation to special subtypes of lymphoma. (*Cancer Sci* 2009; 100: 54–61)

Rituximab is a chimeric monoclonal antibody that has recently been incorporated into the treatment of B-cell non-Hodgkin lymphoma (B-NHL). It recognizes the CD20 antigen, a pan-B-cell marker, binds to it, and induces apoptosis of CD20-positive cells.[1–4] Rituximab can be used as a monotherapy or in combination with conventional chemotherapy for treatment of low- and high-grade, untreated, relapsed, or refractory CD20-positive B-NHL, achieving a high response rate with a low toxicity.

Recent studies have reported that B-NHL show CD20-negative relapse after rituximab therapy.[5–17] Transformation of follicular lymphoma (FL) to CD20-negative diffuse large B-cell lymphoma (DLBCL),[15] proliferation of CD20-negative plasmacytoid tumor cells of marginal zone B-cell lymphoma (MZBCL)[16] or lymphoplasmacytic lymphoma,[13] transformation of FL to classical Hodgkin's lymphoma,[17] and progression of nodular lymphocyte-predominant Hodgkin lymphoma to CD20-negative T-cell-rich B-cell lymphoma have also been reported.[18]

Several mechanisms of resistance to rituximab have been suggested, including selection of a CD20-negative clone as a consequence of rituximab exposure, masking of CD20 epitopes by rituximab itself, or true loss of CD20 antigen by genetic and epigenetic changes.[12,13,15,19–24]

In the present study we carried out retrospective analyses of histological and immunophenotypic changes and outcome in 59 patients with B-NHL after rituximab-containing therapy, to explore the effect of rituximab on CD20 expression and morphology in B-NHL.

Materials and Methods

Patient selection. We reviewed the pathology archives of the National Cancer Center Hospital, Tokyo, Japan, for the period 2002 to 2007. Fifty-nine consecutive cases of CD20-positive B-NHL treated with rituximab, with or without chemotherapy, for which pre- and post-rituximab specimens were available, were included in our study. Rituximab (Zenyaku Kogyo, Tokyo, Japan) was used at a standard dose of 375 mg/m^2 once a week for rituximab monotherapy and once every 3 weeks for the rituximab-cyclophosphamide, doxorubicin, vincristine and prednisone (CHOP) regimen. Clinical information was extracted from the medical records, and the Ann Arbor system was used for staging.

Histological review. Biopsy or surgical specimens were fixed in 10% neutral-buffered formalin overnight, embedded in paraffin, cut into sections 4 μm thick, and stained with hematoxylin–eosin for histological evaluation. All of the pre-rituximab specimens were CD20-positive B-NHL by definition, and post-rituximab specimens included any lymphomas. All of the specimens were reviewed by three pathologists (A.M.M., H.T., and Y.M.) to confirm that the morphological characteristics fulfilled the criteria of the World Health Organization classification of lymphoid neoplasms, 2001.[25] Histological subtype, loss of CD20 expression by immunohistochemistry or flow cytometry, presence or absence of plasmacytoid differentiation, and the relationship between histological transformation and CD20 loss were examined.

Immunohistochemistry, flow cytometry, *in situ* hybridization, and interphase fluorescence *in situ* hybridization analyses. We carried out immunohistochemical staining on formalin-fixed paraffin-embedded pre- and post-rituximab specimens using a panel of monoclonal and polyclonal antibodies. Sections 4 μm thick were cut from each paraffin block, deparaffinized, and incubated

[4]To whom correspondence should be addressed. E-mail: akmaeshi@ncc.go.jp

doi: 10.1111/j.1349-7006.2008.01005.x

at 121°C in pH 6.0 citrate buffer for 10 min for antigen retrieval. Antibodies included those against the following antigens: CD3 (clone PS1, ×25; Novocastra, Newcastle, UK; polymer method), CD20 (L26, ×100; Dako, Glostrup, Denmark; labeled streptavidin–biotin method [LSAB]), and CD79a (JCB117, ×100; Dako; LSAB) routinely; and CD5 (4C7, ×50, Novocastra; polymer), CD7 (CD7-272, ×100; Novocastra; avidin–biotin complex method [ABC]), CD10 (56C6, ×50; Novocastra; polymer), CD15 (MMA, ×100; Becton Dickinson, Franklin Lakes, NJ, USA; polymer), CD30 (Ber-H2, ×100; Dako; polymer), CD45 (2B11 + PD7/26, ×100; Dako; LSAB), CD45RO (UCHL1, ×50; Dako; LSAB), CD56 (1B6, ×100; Novocastra; LSAB), ALK (ALK1, ×200; Dako; polymer), Bcl-2 (124, ×100; Dako; LSAB), Bcl-6 (poly, ×50; Dako; ABC), cyclin D1 (SP4, ×25; Nichirei, Tokyo, Japan; polymer), TIA-1 (26gA10F5, ×1000; Immunotech, Marseille, France; polymer), granzyme B (GrB-7, ×200; Dako; polymer), MPO (poly, ×1000; Dako; LSAB), MUM1 (MUM1p, ×50; Dako; ABC), PAX5 (24, ×200; Becton Dickinson; ABC), TdT (poly, ×100; Dako; polymer), Ig (poly, ×20 000; Dako; LSAB), Ig (poly, ×40 000; Dako; LSAB), IgA (poly, ×100 000; Dako; polymer), IgG (poly, ×20 000; Dako; polymer), and IgM (poly, ×20 000; Dako; polymer) optionally. The percentages of CD20-positive tumor cells were counted semiquantitatively by immunohistochemistry (IHC). Immunoreactivity for CD20 was judged positive (no CD20 loss) if >95% of the tumor cells were stained, partially negative (partial CD20 loss) if 10–95% of the cells were stained, or negative (CD20 loss) if <10% of the cells were stained. When a post-rituximab specimen showed loss of CD20 expression, it was judged as B-cell lineage if there was positivity for CD79a.

Flow cytometry was carried out using an Epics XL-MCL instrument with System II Software (Beckman Coulter). The flow cytometry panel included CD20 (B-Ly1), CD19 (HD37), Ig (poly), and Ig (poly) (Dako). Fluorescence *in situ* hybridization (FISH) and *in situ* hybridization (ISH) analyses were optional. Sections 4 μm thick were cut from each paraffin block and used for FISH analysis. Judgment of the fusion gene was carried out as described previously.[26] Dual-color LSI IGH Spectrum Green/LSI BCL2 Spectrum Orange Dual Fusion Translocation Probes (Vysis, Downers Grove, IL, USA) were used to detect t(14;18): IGHBCL2 fusion. ISH with Epstein–Barr-encoded RNA (EBER-1) probes (Dako) was carried out in some cases to detect possible Epstein–Barr virus infection.

Statistical analysis. The relationships between CD20 expression and treatment regimen (rituximab monotherapy vs combination therapy with rituximab and chemotherapy), response (complete response [CR] vs others, or overall response [OR] vs others), frequency of rituximab administration, and interval between the last dose of rituximab and rebiopsy were examined by ^{2}-test or Mann-Whitney *U*-test. Differences were considered significant when the *P*-value was less than 0.05.

Results

Patient characteristics. Clinical information for all consecutive 59 patients is summarized in Table 1. The patients comprised 32 men and 27 women, ranging in age from 37 to 80 years with a median age of 59 years. Eight patients had stage I/II disease and 51 patients had stage III/IV disease. All of the patients received rituximab by definition, with or without chemotherapy (CHOP or other types of regimen). The 59 patients received a median of six courses (range 1–17) of rituximab. The median interval between the last dose of rituximab and rebiopsy was 6 months (range 4 days to 59 months). The overall response rate was 79% and the % CR was 46% to rituximab-containing regimens.

Four histological patterns of CD20 loss. The results of histological analysis and immunohistochemical staining for each antibody are summarized in Tables 1–2. The total of 59 pre-rituximab B-NHL specimens included 34 FL with or without a DLBCL component, 11 DLBCL, 10 mantle cell lymphomas (MCL), two MZBCL, and two chronic lymphocytic leukemias (CLL). We considered that the following two factors may have contributed to case selection bias. The first factor is that the date of the approval of rituximab for low-grade B-cell lymphoma preceded that for DLBCL for 2 years in Japan. The second factor is that FL were rebiopsied more frequently than DLBCL because FL relapsed frequently and were followed up for a long time, and checks for transformation to DLBCL were sometimes necessary.

Sixteen cases (27%) showed loss of CD20 expression in post-rituximab specimens by IHC or flow cytometry. The frequencies of CD20 loss in the various histological subtypes were: FL, 26% (9/34); DLBCL, 36% (4/11); MCL, 0% (0/10); MZBCL, 50% (1/2); and CLL, 100% (2/2). Among them, two DLBCL and two FL showed partial loss of CD20 expression. Among the 12 tumors with complete loss of CD20 expression, seven had available flow cytometry data, and all of them showed loss of CD20.

Four patterns of loss of CD20 expression were evident (Table 2): pattern 1, CD20 loss with no remarkable histological change (FL, 5; DLBCL, 3; and CLL, 2) (Fig. 1); pattern 2, proliferation of plasmacytoid cells (FL, 2; DLBCL, 1; and MZBCL, 1) (Fig. 2); pattern 3, transformation to classical Hodgkin lymphoma (FL, 1); and pattern 4, transformation to anaplastic large cell lymphoma (ALCL)-like undifferentiated lymphoma (FL, 1) (Fig. 3). All of the lymphomas after rituximab treatment with pattern 1 or 2 histology were positive for CD79a. Two FL with pattern 2 showed proliferation of plasmacytoid cells, not in the marginal zone but in follicles, as with FL with plasma cells,[27,28] and the plasmacytoid tumor cells were positive for IgM and Ig by IHC. One DLBCL with pattern 2 was negative for IgM and Ig by IHC in the pre-rituximab specimen, but positive for them in the post-rituximab specimen. Hodgkin lymphoma with pattern 3, which was previously reported to be a form of transformed FL,[29] was positive for CD30, CD15, and the IGH–BCL2 fusion by FISH, and negative for CD10, CD20, and EBER-1 by ISH. Although we could not determine the lineage of ALCL-like undifferentiated lymphoma with pattern 4, because it was positive for only CD45 and CD45RO and negative for CD3, CD5, CD7, CD10, CD15, CD20, CD30, CD56, CD79a, ALK, bcl-2, bcl-6, granzyme B, MPO, MUM1, PAX5, TdT, TIA-1, and EBER-1 by ISH, it was considered to be transformed FL because of the presence of the IGHBCL2 fusion revealed by FISH in both the pre- and post-rituximab specimens (Fig. 3).

Relationship between rituximab therapy and CD20 expression, and histological changes. The relationships between CD20 expression and interval after the last dose of rituximab, treatment regimens, clinical response, and frequency of rituximab administration were not detected. Among 16 cases showing loss of CD20, the clinical response to treatment was no change (NC) in three cases, and CR or partial response (PR) in the others.

Fourteen patients underwent rebiopsy within 1 month of the last dose of rituximab. Among them, only three cases (21%) were negative for CD20. Seven cases showing loss of CD20 expression after rituximab therapy were subsequently observed and rebiopsied and, among them, two cases (cases FL4-2 and FL8) regained CD20 expression at 7 and 15 months after the last dose of rituximab. The other five cases were found not to have regained CD20 expression at 2, 7, 12, 28, and 44 months after the last dose of rituximab.

Nine patients with FL achieved CR or PR after treatment with a rituximab-containing regimen, but their lymphomas showed early relapse (within 3 months to 1 year later). Among them, five cases (cases FL12, FL18, FL25, FL33, and FL34) relapsed as CD20-positive DLBCL, two (cases FL16 and FL21) as CD20-positive low-grade FL, one (case FL3-2) as CD20-negative FL grade 2, and one (case FL8) as transformation to Hodgkin's lymphoma.

Table 1. Patient characteristics

Case	Age (years)/sex	Stage	Pre-rituximab diagnosis (sample)	Therapy and response between biopsy and operation	Post-rituximab diagnosis (sample)	Post-rituximab interval (months)†	CD20 expression (%)	Histology by immunohistochemistry	Pattern
FL1	55/M	4	FL, gr.2 (LN)	Rx4, NC	FL, gr.1 (BM)	3	0	NHC	1
FL2	52/M	4	FL, gr.2 (LN)	C-MOPPx8, PR, Rx4, NC	FL, gr.1 (BM)	22	0	NHC	1
FL3-1	52/M	3	FL, gr.1 (LN)	R-CHOPx6, CR	FL, gr.2 (BM)	33	100	NHC	
FL3-2				Rx8+C-MOPPx5, CR, relapse, R-ICEx2, PR	FL, gr.2 (LN)	6	0	NHC	1
FL4-1	42/F	4	FL, gr.1 (LN)	Rx8+C-MOPPx16, NC	FL, gr.1 (BM)	23	100	NHC	
FL4-2				Rx8, NC	FL, gr.1 (BM)	5 days	0	NHC	1
FL5	59/M	4	FL, gr.2 (LN)	Rx4, NC, C-MOPPx13, PD, R-C-MOPPx8, CR	FL, gr.2 (BM)	21	–‡	NHC	1
FL6	40/M	4	FL, gr.1 (LN)	R-CHOPx6, CR	FL, gr.2 (LN)	12	90	Partially plasmacytoid cells (IgM+/Ig +/CD138–)	2
FL7	49/F	4	FL, gr.1 (duodeunum)	R-CHOPx6, CR	FL, gr.1 (LN)	17	90	Partially plasmacytoid cells (IgM+/Ig +/CD138–)	2
FL8	61/F	4	DLBCL+FL, gr.3a (LN)	Rx4+CHOPx8, CR	HL, MC (LN)	11	0	Transformation to HL	3
FL9	68/M	4	FL, gr.2 (LN)	R-C-MOPPx6, R-C-MOPPx8, relapse, fludarabine + Rx3	ALCL-like (liver)	18 days	0	Transformation to ALCL-like	4
L10	76/F	4	FL, gr.2 (LN)	Rx8, NC	FL, gr.2 (BM)	6	100	NHC	
FL11	54/F	4	FL, gr.2 (LN)	R-CHOPx6, CR	FL, gr.1 (BM)	15 days	100	NHC	
FL12	40/F	4	FL, gr.1 (LN)	CHOPx6, CR, relapse, C-MOPPx4, NC, Rx4, CR	DLBCL (colon)	4	100	Transformation to DLBCL	
FL13	44/M	4	FL, gr.2 (LN)	R-CHOPx6, PR, C-MOPPx6 radiation, PR	DLBCL+FL, gr.1 (BM)	59	100	Transformation to DLBCL	
FL14	47/M	4	FL, gr.2 (LN)	COPPx6, NC, Rx4, PD	FL, gr.1 (BM)	1	100	NHC	
FL15	43/M	4	FL, gr.1 (LN)	Rx4+C-MOPPx2, CR, zevalin, CR	FL, gr.1 (orbit)	26	100	NHC	
FL16	61/F	4	FL, gr.1 (BM), DLBCL (skin)	R-CHOPx8, CR	FL, gr.2 (LN)	9	100	NHC	
FL17	48/F	4	FL, gr.2 (LN)	Rx4+CHOPx6, PR	FL, gr.1 (BM)	23	100	NHC	
FL18	60/F	3	FL, gr.2 (LN)	Rx4, CR	DLBCL (tonsil)	4	100	Transformation to DLBCL	
FL19	54/F	4	FL, gr.1 (BM, stomach)	R-CHOPx6, PR	FL, gr.1 (BM)	37	100	NHC	
FL20	54/F	4	FL, gr.1 (LN)	Rx4, PR, CHOPx8, PR	FL, gr.2 (cecum)	36	100	NHC	
FL21	61/F	4	FL, gr.2 (LN)	R-CHOPx8, PR	FL, gr.1 (BM)	5	100	NHC	
FL22	66/F	3	FL, gr.2 (LN)	R-CHOPx8, PR	FL, gr.2 (skin)	26	100	NHC	
FL23	53/F	4	FL, gr.2 (ileum, colon)	R-CHOPx8, NC	FL, gr.1 (duodenum)	10	100	NHC	
FL24	51/F	4	FL, gr.2 (duodenum)	Rx1 (within R-CHOP)	FL, gr.1 (duodenum)	4 day	100	NHC	
FL25	55/M	3	DLBCL+FL, gr.3b (LN)	R-CHOPx8, CR	DLBCL (LN)	3	100	NHC	
FL26	37/M	4	FL, gr.2 (LN)	Rx2 (within R-CHOP)	FL, gr.2 (duodenum)	8 days	100	NHC	
FL27	62/M	4	FL, gr.1 (ileum)	Rx3 (within R-CHOP)	FL, gr.1 (duodenum)	8 days	100	NHC	
FL28	57/F	4	FL, gr.3a (LN)	Rx4, NC	DLBCL (LN)	3	100	Transformation to DLBCL	
FL29	51/M	3	DLBCL+FL, gr.3b (LN)	R-CHOPx6+Rx8, CR	DLBCL (LN)	21 days	100	NHC	
FL30	60/M	1	FL, gr.1 (duodenum)	Rx8, CR	FL, gr.1 (duodenum)	4 days	100	NHC	
FL31	63/M	1	FL, gr.1 (duodenum)	Rx8, PR	FL, gr.1 (duodenum)	1	100	NHC	
FL32	75/F	4	FL, gr.1 (BM)	Rx3	FL, gr.1 (BM)	4 days	100	NHC	
FL33	77/M	4	DLBCL+FL, gr.3a (pharynx)	R-CHOPx8, CR	DLBCL (LN)	8	100	NHC	

doi: 10.1111/j.1349-7006.2008.01005.x

Table 1. Continued

Case	Age (years)/sex	Stage	Pre-rituximab diagnosis (sample)	Therapy and response between biopsy and operation	Post-rituximab diagnosis (sample)	Post-rituximab interval (months)†	CD20 expression (%)	Histology by immunohistochemistry	Pattern
FL34	65/M	3	FL, gr.3a (LN)	Rx8, CR	DLBCL (LN)	5	100	Transformation to DLBCL	
DLBCL1-1	47/M	2	DLBCL (right testis)	R-CHOPx8, CR	DLBCL (left testis)	2	100	NHC	
DLBCL1-2				R-IVACx3, CR, BMT, CR	DLBCL (BM)	4	0	NHC	1
DLBCL2	71/M	3	DLBCL (ileum)	R-CHOPx8, CR, Rx1	DLBCL (LN)	10 days	10	NHC	1
DLBCL3	55/M	4	DLBCL (tonsil)	R-CHOPx8, PR	DLBCL (LN)	3	70	NHC	1
DLBCL4	58/F	2	DLBCL (EBER-1+) (stomach)	R-CHOPx8, PR	DLBCL (stomach)	4	0	Plasmacytoid cells (IgM+/Ig +/CD138–)	2
DLBCL5	80/M	2	DLBCL (LN)	R-CHOPx8, CR	DLBCL (subcutaneous)	6	100	NHC	
DLBCL6	60/F	4	DLBCL (breast)	Chemotherapy, Rx4, CR	DLBCL (breast)	29 days	100	NHC	
DLBCL7	61/F	2	DLBCL (tonsil)	R-EPOCHx4, CR	DLBCL (colon, rectum)	16	100	NHC	
DLBCL8	75/F	4	DLBCL (stomach,duodenum)	R-CHOPx8, CR	DLBCL (stomach, duodenum)	30	100	NHC	
DLBCL9	65/F	3	DLBCL (LN)	Rx8+CHOPx6, PD	DLBCL (LN)	3	100	NHC	
DLBCL10	64/M	2	DLBCL (stomach)	Rx1+CHOPx2 (within R-CHOP)	DLBCL (stomach)	20 days	100	NHC	
DLBCL11	63/M	2	DLBCL (LN)	Rx8+CHOPx5+radiation, CR	DLBCL (LN)	8	100	NHC	
MCL1	72/M	4	MCL (LN)	R-CHOPx4, PR, Rx4, NC, COPx6, PD, R-CNOPx6, PD, cladribine, PD	MCL (stomach)	10 days	100	NHC	
MCL2	76/M	4	MCL (LN)	R-CHOPx8, PR	MCL (BM)	20	100	NHC	
MCL3	68/M	4	MCL (BM)	Rx1+CHOPx6, PR	MCL (BM)	1	100	NHC	
MCL4	66/M	4	MCL (colon)	R-CHOPx8, CR	MCL (stomach)	30	100	NHC	
MCL5	55/M	4	MCL (tonsil)	Rx4, PR	MCL (tongue)	28	100	NHC	
MCL6	59/F	4	MCL (stomach)	Rx4, PR, C-MOPPx8+ radiation+COP, PD	MCL (bone)	21	100	NHC	
MCL7-1	63/F	4	MCL (LN)	Rx4+C-MOPPx8, CR	MCL (stomach, duodenum)	17	100	NHC	
MCL7-2				Rx4, PR	MCL (stomach)	1	100	NHC	
MCL8	54/F	4	MCL (ileum)	Rx8+CHOPx6, CR	MCL (small intestine)	3	100	NHC	
MCL9	78/M	4	MCL (stomach)	Rx8, PD	MCL (orbit)	2	100	Change to blastoid variant	
MCL10	70/M	4	MCL (LN)	R-CHOPx8, PR	MCL (stomach)	18	100	NHC	
MZBCL1	68/F	3	MZBCL (LN)	R-ICEx1, CR	MZBCL (tonsil)	15	0	Plasmacytoid cells	2
MZBCL2	55/M	4	MZBCL (BM)	R-CHOPx6, PR	MZBCL (BM)	4	100	NHC	
CLL1	54/M	4	CLL (BM)	Rx2+C-MOPPx6, PR	CLL (LN)	12 days	0	NHC	1
CLL2	52/F	4	CLL (BM)	CHOPx8, COPx10, R-CEPPx7, R-ESHAPx2, CHASEx2, R-ESHAP+PBSCT, Rx5, PR	CLL (BM)	11	0	NHC	1

†From last dose of rituximab; ‡by flow cytometry. ALCL, anaplastic large cell lymphoma; BM, bone marrow; BMT, bone marrow transplantation; CEPP, cyclophosphamide, etoposide, procarbazine, and prednisolone; CHASE, cyclophosphamide, cytosine arabinoside, etoposide, and dexamethasone; CHOP, cyclophosphamide, doxorubicin, vincristine, and prednisone; CLL, chronic lymphocytic leukemia; C-MOPP, cyclophosphamide, vincristine, prednisone, and procarbazine; CR, complete response; diff., differentiation; DLBCL, diffuse large B-cell lymphoma; EPOCH, etoposide, prednisone, vincristine, cyclophosphamide, and doxorubicin; ESHAP, etoposide, methylprednisolone, high-dose cytarabine, and cisplatin; FL, follicular lymphoma; HL, Hodgkin's lymphoma; ICE, ifosfamide, carboplatin, and etoposide; IVAC, ifosfamide, vincristine, and cytarabine; LN, lymph node; MC, mixed cellularity; MCL, mantle cell lymphoma; MZBCL, marginal zone B-cell lymphoma; NC, no change; NHC, no remarkable histological change; PBSCT, peripheral blood stem cell transplantation; PD, progressive disease; PR, partial response; R, rituximab.

Cancer Sci | January 2009 | vol. 100 | no. 1 | 57

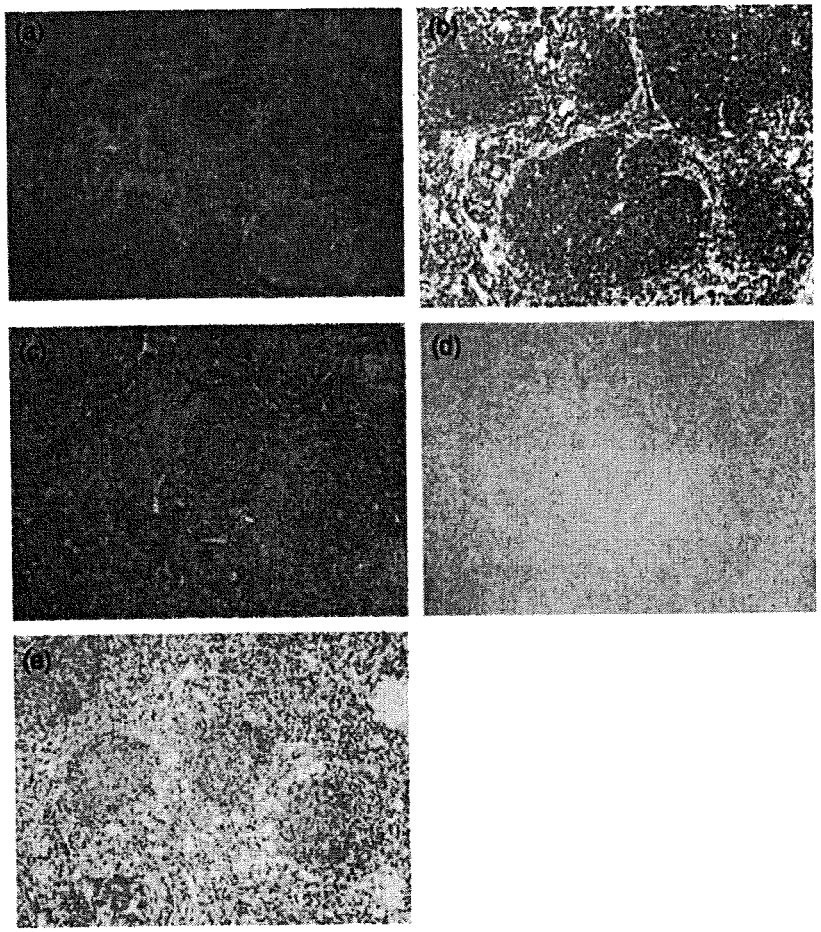

Fig. 1. (a–e) A case of pattern 1 change in CD20-positive follicular lymphoma (FL) to CD20-negative FL. FL, grade 1, (a) in a lymph node (hematoxylin–eosin, ×40) and (b) with CD20-positive phenotype, pre-rituximab (×100). FL, grade 2, (c) in a lymph node (hematoxylin–eosin, ×40) with (d) CD20-negative (×40) and (e) CD79a-positive (×40) phenotypes, post-rituximab.

Table 2. Four histological patterns of loss of CD20 expression after rituximab therapy

Histological pattern	Distribution
Pattern 1: loss of CD20 with no remarkable histological change	FL, 5; DLBCL, 3; CLL, 2
Pattern 2: proliferation of plasmacytoid cells	FL, 2; DLBCL, 1; MZBCL, 1
Pattern 3: transformation to classical Hodgkin lymphoma	FL, 1
Pattern 4: transformation to anaplastic large cell lymphoma-like undifferentiated lymphoma	FL, 1

CLL, chronic lymphocytic leukemia; DLBCL, diffuse large B-cell lymphoma; FL, follicular lymphoma; MZBCL, marginal zone B-cell lymphoma.

Discussion

Recent reports have indicated that the treatment of B-NHL with rituximab may be associated with CD20-negative lymphoma relapse,[5–17] and the frequency of loss of CD20 after rituximab treatment varies widely (24, 56, 60, and 94%).[9,11,13,14] In the present study, 16 of 59 B-NHL (27%) showed loss of CD20 after rituximab-containing therapy using a larger series than in previous reports. Our results also suggested that the frequency of CD20 loss was not largely affected by the period before rebiopsy. Although the site of sampling (bone marrow vs non-bone marrow) might affect the observed degree of CD20 loss,[9] this issue needs to be studied further using a larger number of cases. Tumors with loss of CD20 in the present study included FL, DLBCL, MZBCL, and CLL. Although Goteri *et al.* reported that MCL frequently showed loss of CD20 expression in bone marrow, none of our MCL cases showed CD20 loss.[13] Because a previous report indicated that rituximab + CHOP combination therapy (R-CHOP) had insufficient efficacy for MCL,[30] it was considered that this regimen might not have been sufficiently potent to induce selection of a CD20-negative clone.

Four histological patterns of CD20 loss were evident. The majority were patterns 1 or 2, whereas patterns 3 or 4 were rare. Recently, several reports have described relapse with pattern 1 or 2 histology after rituximab therapy.[13,16] Using flow cytometry, Goteri *et al.* demonstrated that 26 cases of low-grade B-cell lymphoma showed CD20 loss in bone marrow aspirates, including cases with no histological change, and with residual plasmacytoid tumor cells of lymphoplasmacytic lymphoma.[13] It has also been reported that mucosa-associated lymphoid tissue lymphoma changes to a pure plasma-cell neoplasm.[16]

Case FL8, which showed transformation to Hodgkin lymphoma (pattern 3), was one of the transformed FL that we reported previously.[29] As composite Hodgkin lymphoma and FL is reported to be very rare,[31,32] rituximab might have induced transformation to Hodgkin lymphoma. Recently, a case

doi: 10.1111/j.1349-7006.2008.01005.x

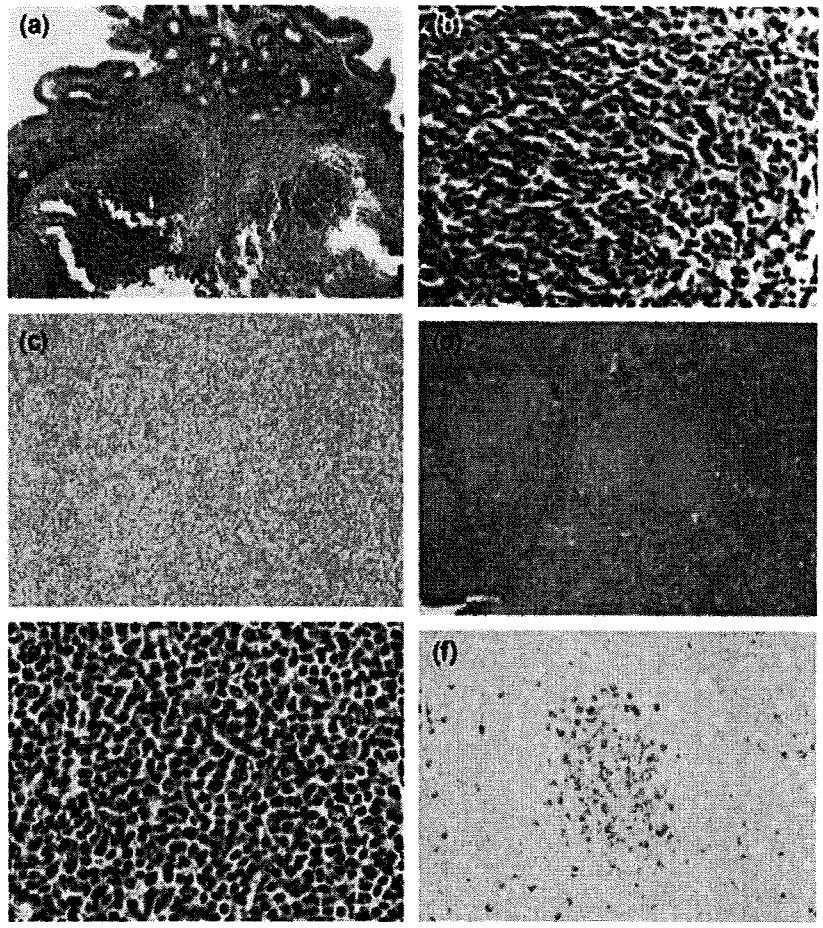

Fig. 2. (a–f) A case of pattern 2 change of follicular lymphoma (FL) to FL with plasma cells. FL, grade 1 in duodenum (hematoxylin–eosin), (a) ×40, (b) ×400, with (c) IgM-negative phenotype (×100), pre-rituximab. FL, grade 1 with plasmacytoid differentiation in lymph node (hematoxylin–eosin), (d) ×40, (e) ×400, with (f) IgM-positive phenotype (×100), post-rituximab.

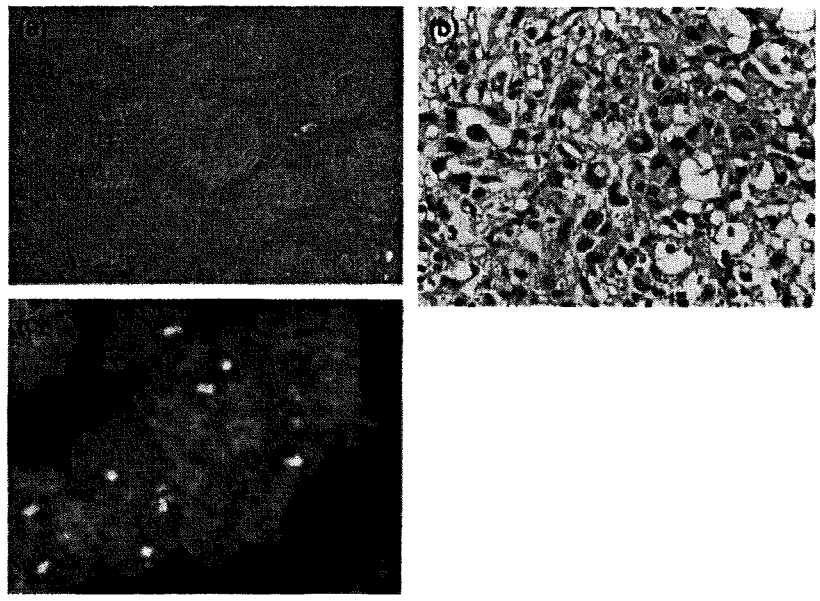

Fig. 3. (a–c) A case of pattern 4 change of follicular lymphoma (FL) to anaplastic large-cell lymphoma (ALCL)-like undifferentiated lymphoma. (a) FL, grade 2 in lymph node, pre-rituximab (hematoxylin–eosin, ×40). (b) ALCL-like undifferentiated lymphoma in liver, post-rituximab (hematoxylin–eosin, ×400). (c) The result of fluorescence *in situ* hybridization of ALCL-like undifferentiated lymphoma. IGH and BCL2 fusion pattern. Two fusion IGHBCL2 signals were present.

of Hodgkin lymphoma subsequent to FL in a patient receiving maintenance rituximab was reported.[17]

Transformation from FL to ALCL-like undifferentiated lymphoma (pattern 4) has been reported previously as neither transformation of FL nor histological change after rituximab therapy. Although two cases of FL with relapse to peripheral T-cell lymphoma after rituximab have been reported,[33,34] it was suspected that the T-cell lymphomas were another clone, thus differing from the present case. Cohen *et al.* reported large-cell transformation of CLL and FL during or soon after treatment with a fludarabine- and rituximab-containing regimen,[35] thus resembling the present case treated with fludarabine and rituximab.

Several mechanisms of resistance to rituximab have been suggested, including selection of a CD20-negative clone as a consequence of rituximab exposure, masking of CD20 epitopes by rituximab itself, or true loss of CD20 antigen due to genetic and epigenetic changes.[12,13,15,19–24] Although the present study was not intended to address the mechanism of CD20 loss, several remarkable phenomena were evident. No relationships were detected between loss of CD20 and the interval between the last dose of rituximab and rebiopsy, frequency of rituximab administration, clinical responses, and treatment regimens. It is suspected that susceptibility to rituximab differs greatly among lymphomas. Our results also indicated that loss of CD20 immediately after rituximab therapy was not frequent. Although some cases do regain CD20 expression, loss of CD20 persisting for more than 6 months is not infrequent.

A previous case report has emphasized that early relapse of FL after rituximab therapy was related to CD20-negative transformation to DLBCL.[15] However, this was not confirmed in our study using a larger series: most of the relapses were CD20-positive DLBCL, and only two were CD20-negative FL or Hodgkin lymphoma. Our results suggested that CD20-positive relapse with histological transformation occurred most frequently in cases of early relapse, and that CD20-negative relapse was relatively rare.

In conclusion, our findings indicate that 27% of B-NHL show loss of CD20 expression with four histological patterns after rituximab therapy. As the changes in morphology and CD20 expression after rituximab therapy vary widely, including not only loss of CD20 expression but also proliferation of plasmacytoid cells or transformation to special subtypes of lymphoma, and clinical outcomes are very confused, careful follow up and rebiopsy are recommended.

Acknowledgments

The authors are grateful to Ms S. Miura and Ms C. Kina for their excellent technical assistance.

References

1 Reff ME, Carner K, Chambers KS *et al.* Depletion of B cells *in vivo* by a chimeric mouse human monoclonal antibody to CD20. *Blood* 1994; 83: 435–45.
2 Demidem A, Lam T, Alas S *et al.* Chimeric anti-CD20 (IDEC-C2B8) monoclonal antibody sensitizes a B cell lymphoma cell line to cell killing by cytotoxic drugs. *Cancer Biother Radiopharm* 1997; 12: 177–86.
3 Shan D, Ledbetter JA, Press OW. Apoptosis of malignant human B cells by ligation of CD20 with monoclonal antibodies. *Blood* 1998; 91: 1644–52.
4 Cardarelli PM, Quinn M, Buckman D *et al.* Binding to CD20 by anti-B1 antibody or F(ab)(2) is sufficient for induction of apoptosis in B-cell lines. *Cancer Immunol Immunother* 2002; 51: 15–24.
5 Meeker T, Lewder J, Cteary ML *et al.* Emergence of idiotype variants during treatment of B-cell lymphoma with anti-idiotype antibodies. *N Eng J Med* 1985; 312: 1658–65.
6 Kinoshita T, Nagai H, Murate T *et al.* CD20-negative relapse in B-cell lymphoma after treatment with rituximab. *J Clin Oncol* 1998; 16: 3916.
7 Davis TA, Czerwinski DK, Levy R. Therapy of B-cell lymphoma with anti-CD20 antibodies can result in the loss of CD20 antigen expression. *Clin Cancer Res* 1999; 5: 611–15.
8 Schmitz K, Brugger W, Weiss B *et al.* Clonal selection of CD20-negative non-Hodgkin's lymphoma cells after treatment with anti-CD20 antibody rituximab. *Br J Haematol* 1999; 106: 571–2.
9 Foran JM, Norton AJ, Micallef IN *et al.* Loss of CD20 expression following treatment with rituximab (chimaeric monoclonal anti-CD20): a retrospective cohort analysis. *Br J Haematol* 2001; 114: 881–3.
10 Chu PG, Chen YY, Molina A *et al.* Recurrent B-cell neoplasms after Rituximab therapy: an immunophenotypic and genotypic study. *Leuk Lymphoma* 2002; 43: 2335–41.
11 Kennedy GA, Tey SK, Cobcroft R *et al.* Incidence and nature of CD20-negative relapses following rituximab therapy in aggressive B-cell non-Hodgkin's lymphoma: a retrospective review. *Br J Haematol* 2002; 119: 412–16.
12 Jilani I, O'Brien S, Manshuri T *et al.* Transient down-modulation of CD20 by rituximab in patients with chronic lymphocytic leukemia. *Blood* 2003; 102: 3514–20.
13 Goteri G, Olivieri A, Ranaldi M *et al.* Bone marrow histopathological and molecular changes of small B-cell lymphomas after rituximab therapy: comparison with clinical response and patients' outcome. *Int J Immunopathol Pharmacol* 2006; 19: 421–31.
14 Seliem RM, Freeman JK, Steingart RH *et al.* Immunophenotypic changes and clinical outcome in B-cell lymphomas treated with rituximab. *Appl Immunohistochem Mol Morphol* 2006; 14: 18–23.
15 Alovaro-Naranjo TA, Jaen-Martinez JJ, Guma-Padro JG *et al.* CD20-negative DLBCL transformation after rituximab treatment in follicular lymphoma: a new case report and review of the literature. *Ann Hematol* 2003; 82: 585–8.
16 Woehrer S, Streubel B, Chott A *et al.* Transformation of MALT lymphoma to pure plasma cell histology following treatment with the anti-CD20 antibody rituximab. *Leuk Lymphoma* 2005; 46: 1645–9.
17 Scaramucci L, Perrotti A, Niscola P *et al.* Hodgkin disease subsequent to follicular lymphoma on maintenance rituximab. *Leuk Lymphoma* 2007; 48: 1878–80.
18 Pijuan L, Vicioso L, Bellosillo B *et al.* CD20-negative T-cell-rich B-cell lymphoma as a progression of a nodular lymphocyte-predominant Hodgkin's lymphoma treated with rituximab: a molecular analysis using laser capture microdissection. *Am J Surg Pathol* 2005; 29: 1399–403.
19 Cragg MS, Bayne MC, Illidge TM *et al.* Apparent modulation of CD20 by rituximab: an alternative explanation. *Blood* 2004; 103: 3989–90.
20 Rawal YB, Nuovo GJ, Frambach GE *et al.* The absence of CD20 messenger RNA in recurrent cutaneous B-cell lymphoma following rituximab therapy. *J Cutan Pathol* 2005; 32: 616–21.
21 Takei K, Yamazaki T, Sawada U *et al.* Analysis of changes in CD20, CD55, and CD59 expression on established rituximab-resistant B-lymphoma cell lines. *Leuk Res* 2006; 30: 625–31.
22 Tomita A, Hiraga J, Kiyoi H *et al.* Epigenetic regulation of CD20 protein expression in a novel B-cell lymphoma cell line, RRBL1, established from a patient treated repeatedly with rituximab-containing chemotherapy. *Int J Hematol* 2007; 86: 49–57.
23 Jazirehi AR, Vega MI, Bonavida B. Development of rituximab-resistant lymphoma clones with altered cell signaling and cross-resistance to chemotherapy. *Cancer Res* 2007; 67: 1270–81.
24 Czuczman MS, Olejniczak S, Gowda A *et al.* Acquirement of rituximab resistance in lymphoma cell lines is associated with both global CD20 gene and protein down-regulation regulated at the pretranscriptional and posttranscriptional levels. *Clin Cancer Res* 2008; 14: 1561–70.
25 Jaffe ES, Harris NL, Stein H *et al. World Health Organization Classification of Tumours Pathology & Genetics: Tumours of Haematopoietic and Lymphoid Tissues*. Lyon: IARC Press, 2001.
26 Sekiguchi N, Kobayashi Y, Yokota Y *et al.* Follicular lymphoma subgrouping by fluorescence *in situ* hybridization analysis. *Cancer Sci* 2005; 96: 77–82.
27 Keith TA, Cousar JB, Glick AD *et al.* Plasmacytic differentiation in follicular center cell (FCC) lymphomas. *Am J Clin Pathol* 1985; 84: 283–90.
28 Vago JF, Hurtubise PE, Redden-Borowski MM *et al.* Follicular center-cell lymphoma with plasmacytic differentiation, monoclonal paraprotein, and peripheral blood involvement: recapitulation of normal B-cell development. *Am J Surg Pathol* 1985; 9: 764–70.
29 Maeshima AM, Omatsu M, Nomoto J *et al.* Diffuse large B-cell lymphoma after transformation from low-grade follicular lymphoma: morphological, immunohistochemical and FISH analyses. *Cancer Sci* 2008; 99: 1760–8.
30 Lenz G, Dreyling M, Hoster E *et al.* Immunochemotherapy with rituximab and cyclophosphamide, doxorubicin, vincristine, and prednisone significantly improves response and time to treatment failure, but not long-term outcome in patients with previously untreated mantle cell lymphoma: results of a

doi: 10.1111/j.1349-7006.2008.01005.x

prospective randomized trial of the German Low Grade Lymphoma Study Group (GLSG). *J Clin Oncol* 2005; **23**: 1984–92.
31 Brauninger A, Hansmann ML, Strickler JG *et al.* Identification of common germinal-center B-cell precursors in two patients with both Hodgkin's disease and non-Hodgkin's lymphoma. *N Eng J Med* 1999; **340**: 1239–47.
32 Marafioti T, Hummel M, Anagnostopoulos I *et al.* Classical Hodgkin's disease and follicular lymphoma originating from the same germinal center B cell. *J Clin Oncol* 1999; **17**: 3804–9.
33 Micallef IN, Kirk A, Norton A *et al.* Peripheral T-cell lymphoma following rituximab therapy for B-cell lymphoma. *Blood* 1999; **93**: 2427–8.
34 Tetreault S, Abler SL, Robbins B *et al.* Peripheral T-cell lymphoma after anti-CD20 antibody therapy. *J Clin Oncol* 1998; **16**: 1635–7.
35 Cohen Y, Da'as N, Libstet D *et al.* Large-cell transformation of chronic lymphocytic leukemia and follicular lymphoma during or soon after treatment with fludarabine-rituximab-containing regimens: natural history- or therapy-related complication? *Eur J Haematol* 2002; **68**: 80–3.

Secondary CD5+ Diffuse Large B-Cell Lymphoma Not Associated With Transformation of Chronic Lymphocytic Leukemia/Small Lymphocytic Lymphoma (Richter Syndrome)

Akiko Miyagi Maeshima, MD,[1] Hirokazu Taniguchi, MD,[1] Junko Nomoto, CT,[2] Dai Maruyama, MD,[2] Sung-Won Kim, MD,[2] Takashi Watanabe, MD,[2] Yukio Kobayashi, MD,[2] Kensei Tobinai, MD,[2] and Yoshihiro Matsuno, MD[3]

Key Words: CD5; Diffuse large B-cell lymphoma; Secondary disease; Immunohistochemistry; Non–Richter syndrome

DOI: 10.1309/AJCP58FETFGLCKKW

Abstract

Few cases of secondary CD5+ diffuse large B-cell lymphoma (DLBCL) that are not Richter syndrome have been reported previously. We report 9 cases of non–Richter syndrome secondary CD5+ DLBCL. Among 529 cases of DLBCL, 38 (7.2%) were CD5+ DLBCL, including 9 of secondary CD5+ DLBCL. Five cases gained CD5 expression during the clinical course of DLBCL (group 1). Three cases showed transformation from CD5– low-grade B-cell lymphoma to CD5+ DLBCL (group 2). The remaining case showed coexistence of CD5+ DLBCL and CD5+ follicular lymphoma. The clonal relationships of CD5– and CD5+ tumors were confirmed in all 4 available cases. Cases of secondary CD5+ DLBCL that were not Richter syndrome were classifiable into 3 groups. Groups 1 and 2 showed the gain of CD5 during the clinical course or transformation of the tumors, suggesting that CD5 expression is closely associated with the progression of B-cell lymphoma.

Diffuse large B-cell lymphoma (DLBCL) is the largest and most widely heterogeneous category of aggressive lymphomas.[1] CD5 expression in DLBCL is currently a focus of clinical and pathologic interest. Richter syndrome, transformation of chronic lymphocytic leukemia/small lymphocytic lymphoma (CLL/SLL), is a well-known form of secondary CD5+ DLBCL, but few cases of secondary CD5+ DLBCL that are not Richter syndrome have been reported previously.

The CD5 molecule is a 67-kDa glycoprotein that is expressed by most T cells and a subset of B cells.[2] Among mature B-cell neoplasms, most cases of CLL/SLL express CD5 and often undergo transformation to CD5+ DLBCL, so-called Richter syndrome. CD5 is also expressed in most cases of mantle cell lymphoma, but less frequently in DLBCL[3-5] and intravascular large B-cell lymphoma[6] and in only a small proportion of cases of extranodal marginal zone B-cell lymphoma,[7,8] Burkitt lymphoma,[9] follicular lymphoma (FL),[10-14] splenic marginal zone B-cell lymphoma,[15] and primary effusion lymphoma.[16] It is speculated that these neoplasms could switch or transform to CD5+ DLBCL, although few reports have indicated that CD5+ FL can transform to CD5+ DLBCL.[13,14] Moreover, apart from 1 case reported previously by our group,[17] transformation of CD5– low-grade B-cell lymphoma to CD5+ DLBCL seems to be rare.

Matolcsy et al[3] highlighted the phenomenon of de novo evolution of CD5 expression in DLBCL that is not a result of transformation, suggesting that such DLBCL is genotypically distinct from Richter syndrome–associated DLBCL. Yamaguchi et al[5] reported that CD5+ DLBCL accounted for approximately 10% of de novo DLBCL cases and that CD5 was a marker of poor prognosis in de novo DLBCL. They indicated that patients with CD5+ DLBCL showed an

older age distribution, a female predominance, poor performance status, a higher level of serum lactate dehydrogenase, advanced stage, a tendency to have more than 1 extranodal site and B symptom, and a higher International Prognostic Index score than patients with CD5– DLBCL. However, there has been no report of secondary CD5+ DLBCL gaining CD5 expression during the clinical course. Herein we report 9 cases of secondary CD5+ DLBCL that were not Richter syndrome.

Materials and Methods

Patient Selection

We reviewed the pathology archives of the National Cancer Center Hospital, Tokyo, Japan, for the period between 2002 and 2007. The total number of patients with DLBCL with or without a low-grade B-cell lymphoma component was 529, and the total number of specimens available was 728 (1-5 per case). Clinical information was extracted from the medical records, and the Ann Arbor system was used for staging.

Morphologic Review

The materials were fixed in 10% neutral-buffered formalin overnight, embedded in paraffin, cut into sections 4 μm thick, and stained with H&E for routine histologic evaluation. All specimens were reviewed by 3 pathologists (A.M.M., H.T., and Y.M.) to confirm that the morphologic characteristics fulfilled the criteria for DLBCL in the 2001 World Health Organization classification of lymphoid neoplasms.[1] When a low-grade B-cell lymphoma component was detected in previous or synchronous specimens, its histologic features were also evaluated. DLBCL was subclassified as the centroblastic, anaplastic, immunoblastic, or T-cell/histiocyte-rich variant. The presence of intravascular involvement, like that seen in intravascular large B-cell lymphoma, was also evaluated.

Immunohistochemical Studies, In Situ Hybridization, Flow Cytometry, and Interface Fluorescence In Situ Hybridization

We performed immunohistochemical analysis on formalin-fixed paraffin-embedded tissue samples by using a panel of monoclonal and polyclonal antibodies. Sections 4 μm thick were cut from each paraffin block, deparaffinized, and incubated at 121°C in citrate buffer, pH 6.0, for 10 minutes for antigen retrieval. Antibodies included those against the following antigens: CD3 (PS1, ×25; Novocastra, Newcastle upon Tyne, England), CD5 (4C7, ×50; Novocastra), CD10 (56C6, ×50; Novocastra), CD20 (L26, ×100; DAKO, Glostrup, Denmark), CD23 (1B12, ×100; Novocastra), bcl-6 (polyclonal, ×50; DAKO, Kyoto, Japan), cyclin D1 (SP4, ×25; Nichirei, Tokyo), MUM1 (MUM1p, ×50; DAKO, Kyoto), and p53 (DO7, ×100; DAKO, Glostrup), using an autostainer with the standard polymer (DAKO Autostainer Plus, Glostrup, for CD3, CD5, CD10, CD23, and cyclin D1) or the labeled streptavidin-biotin method (BioGenex Autostainer, San Ramon, CA, for CD20 and p53) or manually by the standard avidin-biotin complex method (bcl-6 and MUM1).

Immunohistochemical analysis for CD3, CD20, and CD5 was performed in all DLBCLs. Immunoreactivity for CD5 was judged positive if more than 20% of the tumor cells were stained. In all specimens of CD5– and CD5+ lymphomas of secondary CD5+ DLBCLs, CD5 was restained by the avidin-biotin complex method simultaneously, and the reproducibility of CD5 expression was confirmed. When a DLBCL had a CD5+ phenotype, the cyclin D1– phenotype was examined. The CD5– DLBCL or CD5– low-grade B-cell lymphoma and CD5+ DLBCL components were stained for CD10, bcl-6, MUM1, CD23, and p53, as well as for CD3, CD20, CD5, and cyclin D1.

To classify each case as having a germinal center B-cell (GCB) phenotype or a non-GCB phenotype, a panel of 3 antigens (CD10, bcl-6, and MUM1) was used according to the protocol reported by Hans et al.[18] All immunohistochemical specimens were judged by one of us (A.M.M.) and confirmed by 2 others (H.T. and Y.M.). In situ hybridization (ISH) with Epstein-Barr virus–encoded RNA (EBER-1) probes (DAKO, Glostrup) was performed to detect possible EBV infection.

Flow cytometry was performed on a Beckman Coulter Epics XL-MCL instrument with System II software (Beckman Coulter, Fullerton, CA). Cells were stained with fluorescein isothiocyanate–labeled antibodies against CD20 (B-Ly1, DAKO, Glostrup) and phycoerythrin-labeled CD5 (DK23, DAKO, Glostrup). The total population of viable cells was gated using forward and right scatter. Double positivity of CD5 and CD20 was defined as 15% or more of the population expressing both markers. The results of flow cytometry and immunohistochemical analysis were compared, and their degrees of agreement were examined.

Interface fluorescence ISH analysis was optional and performed on sections 4 μm thick cut from each paraffin block. Judgment of the fusion gene was performed as described previously.[19] Dual-color LSI IGH Spectrum Green/LSI BCL2 Spectrum Orange Dual Fusion Translocation Probes (Vysis, Downers Grove, IL) were used to detect *IGH/BCL2* fusion.

Polymerase Chain Reaction and Sequencing

DNA was extracted from paraffin-embedded tissue sections by using the DNA Micro Kit (Qiagen, Tokyo). To amplify the rearranged immunoglobulin heavy chain variable region gene, *CDR3,* we performed seminested polymerase chain reaction (PCR) using primers directed at consensus sequences of framework 3 (Fr3A, 5′-ACA CGG C(C/T)(G/C) TGT ATT ACT GT-3′) of the variable region and common sequence of the joining region (LJH, 5′-TGA GGA GAC

DOI: 10.1309/AJCP58FETFGLCKKW

GGT GAC C-3′ and VLJH, 5′-GTG ACC AGG GTN CCT TGG CCC CAG-3′). All PCR reactions were performed in 20-μL total volumes under standard conditions using LA *Taq* polymerase (Takara Bio, Shiga, Japan).

The amplified products were electrophoresed on 3% polyacrylamide gels. In cases with a monoclonal band, PCR products were purified by using Microcon YM-100 (Millipore, Bedford, MA). PCR amplification was performed by using the BigDye Terminator Cycle Sequencing Kit (Applied Biosystems, Foster City, CA), and automated fluorescent sequencing was performed on an ABI prism 310-Avant Genetic Analyzer (Applied Biosystems).

Results

Characteristics of Patients With Non–Richter Syndrome Secondary CD5+ DLBCL

There were 38 cases of CD5+ DLBCL (7.2%), among which 9 cases of secondary CD5+ DLBCL were identified (9/38 [24%]). None of the cases was Richter syndrome. Clinical information is summarized in **Table 1**. The patients comprised 6 men and 3 women, ranging in age from 24 to 76 years with a median age of 63 years. Six patients had stage I or II disease, and 3 had stage III or IV disease at initial diagnosis. All patients received chemotherapy (cyclophosphamide, doxorubicin, vincristine, and prednisone or other types of regimen). The 5-year overall survival from initial diagnosis was 80%.

Three Histologic Groups of Secondary CD5+ DLBCL

The 9 cases of non–Richter syndrome secondary CD5+ DLBCL were classifiable into 3 groups. In the 8 cases constituting group 1 (gained CD5 expression during the clinical course of DLBCL, 5 cases) and group 2 (showed transformation from CD5– low-grade B-cell lymphoma to CD5+ DLBCL, 3 cases), the biopsy sites of CD5– B-cell non-Hodgkin lymphoma at initial diagnosis were lymph node (2), Waldeyer ring (1), and extranodal sites (5, 1 each in breast, bone marrow, maxillary sinus, orbit, and small intestine). The biopsy sites of the CD5+ DLBCLs were lymph node (5), tonsil (1), and extranodal sites (2, 1 each in skin and soft tissue). The single tumor constituting group 3 (case 9) was obtained

Table 1
Patient Characteristics in 9 Cases of Secondary CD5+ Diffuse Large B-Cell Lymphoma

Case No./ Sex/Age(y)	Months After Diagnosis	Histologic Type	CD5*	Biopsy Site	PS	Stage	IPI	LDH (U/L)†	EN	B Symptoms	Postbiopsy Therapy/Response	Follow-up (mo)/ Outcome
1/F/62	0	DLBCL	–	Breast	0	I	LI	506	0	–	CHOP ×6 and RT, 40 Gy/CR	
	37	DLBCL	+	Cervical LN							R-C-MOPP ×6 and RT, 40 Gy/CR	
	56	DLBCL	+	Inguinal LN							R ×1 and ESHAP ×3	58/AWD
2/F/63	0	DLBCL	–	Maxillary sinus	0	II	L	146	1	–	CHOP ×6, IT ×3, and RT, 46 Gy/PR	
	7	DLBCL	+	Cervical LN							EPOCH ×1/PD; IVAC ×1, and CODOX-M ×2/PD; R ×3/NC	13/AWD
3/M/24	0	DLBCL	–	Waldeyer ring	0	II	L	127	1	–	R ×4, CHOP ×6, and RT, 40 Gy/CR	
	8	DLBCL	+	Soft tissue							IT, RT at 30 Gy, R ×5, and IVAC ×3/PR; BMT	24/DOD
4/M/63	0	DLBCL	–	Cervical LN	0	II	L	209	0	–	R-CHOP ×6 and RT, 40 Gy/CR	
	15	DLBCL	+	Inguinal LN							Auto-PBSCT	19/AWOD
5/M/66	0	DLBCL	NA	Abdominal LN	0	IV	HI	305	2	–	CHOP ×8/CR	
	48	DLBCL	–	Prostate							EPOCH ×4/CR	
	75	DLBCL	+	Skin							RT, 35 Gy, and R-C-MOPP	77/AWD
6/M/47	0	FL, grade 2	–	Small intestine	0	II	L	150	1	–	CHOP ×8/CR; C-MOPP ×4 and RT, 40 Gy/CR	
	75	DLBCL	+	Tonsil							ESHAP ×3 + R ×8, R-ICE ×4	123/DOD
7/M/69	0	MALT lymphoma	–	Orbit	0	IV	H	439	2	–	R ×1, C-MOPP ×14, and VDS and C-MOPP ×6/PR	
	56	DLBCL	+	Abdominal LN								57/AWD
8/F/76	0	LPL	–	BM	2	IV	H	750	1	+	CHOP ×2/PD; R-ESHAP ×1/PR	
	0	DLBCL	+	Cervical LN								5/AWD
9/M/27	0	DLBCL and FL, grade 3b	+	Cervical LN	0	I	L	172	0	–	R ×8 , CHOP ×3 , RT, and 30 Gy/CR	2/AWOD

AWD, alive with disease; AWOD, alive without disease; BM, bone marrow; BMT, bone marrow transplantation; CHOP, cyclophosphamide, doxorubicin, vincristine, and prednisone; C-MOPP, cyclophosphamide, vincristine, prednisone, and procarbazine; CODOX-M, cyclophosphamide, doxorubicin, and high-dose methotrexate; CR, complete remission; DLBCL, diffuse large B-cell lymphoma; DOD, died of disease; EN, number of extranodal sites; EPOCH, doxorubicin, vincristine, etoposide, cyclophosphamide, and prednisone; ESHAP, etoposide, carboplatin, cytarabine, and methylprednisolone; FL, follicular lymphoma; H, high; HI, high intermediate; ICE, ifosfamide, carboplatin, and etoposide; IPI, International Prognostic Index; IT, intrathecal methotrexate and prednisolone; IVAC, ifosfamide, etoposide, and high-dose cytarabine; L, low; LDH, serum lactate dehydrogenase; LI, low intermediate; LN, lymph node; LPL, lymphoplasmacytic lymphoma; MALT, mucosa-associated lymphoid tissue; NA, not available; NC, no change; PBSCT, peripheral blood stem cell transplantation; PD, progressive disease; PR, partial remission; PS, performance status; R, rituximab; RT, radiotherapy; VDS, vindesine, doxorubicin, and prednisone.

* By immunohistochemical analysis.

† The reference range for all cases except case 5 is 119-229 U/L; for case 5, it is 260-420 U/L. Values are given in conventional units; to convert to Système International units (μkat/L), multiply by 0.0167.

from a lymph node. Table 1 and ▮Table 2▮ summarize the clinicopathologic findings.

The 5 cases in group 1 gained CD5 during the clinical course of DLBCL ▮Image 1▮. CD5– DLBCL was the initial diagnosis presentation, and CD5 expression was 0% by immunohistochemical analysis. CD5+ DLBCL was the diagnosis at relapse, 7, 8, 15, 27, and 37 months after the initial diagnosis of CD5– DLBCL, respectively.

The 3 cases in group 2 gained CD5 throughout transformation of CD5– low-grade B-cell lymphoma to DLBCL. The initial diagnoses were CD5– FL grade 2, CD5– mucosa-associated lymphoid tissue (MALT) lymphoma, and CD5– lymphoplasmacytic lymphoma (LPL), and they transformed to CD5+ DLBCL. The case that showed transformation of CD5– FL to CD5+ DLBCL has been reported previously by our group.[17] Although this FL case had a CD10+/CD5– phenotype in an FL component and a CD10–/CD5+ phenotype in a DLBCL component, *IGH/BCL2* fusion was detected in both components, suggesting that transformation to CD5+ DLBCL had occurred. The patient with CD5– MALT lymphoma had stage IV disease at initial diagnosis, and, after 56 months, CD5+ DLBCL was diagnosed in an abdominal LN.

In the LPL case ▮Image 2▮, multiple lymphoid cell aggregates with plasmacytoid differentiation were detected in a bone marrow aspiration specimen. This was diagnosed as low-grade B-cell lymphoma with plasmacytoid differentiation having a cytoplasmic IgM+ phenotype. The tumor extended to the general lymph nodes and bone marrow but involved no other sites, including the peripheral blood or spleen. The serum IgM level was high at 895 mg/dL. On the basis of this information, we diagnosed the disease as LPL. There was synchronous CD5+ DLBCL in the cervical lymph node.

The case constituting group 3 showed coexistence and gradual shift of CD5+/CD10+ FL grade 3b to CD5+/CD10+ DLBCL in the cervical lymph node.

Immunohistochemical Studies, ISH, and Clonality Analysis for Secondary CD5+ DLBCL

All specimens were negative for cyclin D1 by immunohistochemical analysis. CD10 and CD23 were both positive

▮Table 2▮
Results of Immunohistochemical, Flow Cytometry, FISH, EBER-1 ISH, and Clonality Analysis in 9 Cases of Secondary CD5+ DLBCL

Case No./ Histologic Subtype	CD20	CD5*	CD5†	Cyclin D1	CD10	CD23	bcl-6	MUM1	GCB/ Non-GCB	p53	EBER-1 ISH	FISH	Clonality
1													
DLBCL, centroblastic	+	– (0)	ND	–	–	–	ND	ND	ND	ND	ND	ND	Related
DLBCL, centroblastic	+	+ (20)	–	–	–	–	+	–	GCB	–	ND	ND	
DLBCL, centroblastic	+	+ (80)	+	–	–	–	+	–	GCB	–	–	ND	
2													
DLBCL, centroblastic	+	– (0)	ND	–	–	ND	ND	ND	ND	ND	ND	ND	ND
DLBCL, centroblastic	+	+ (100)	+	–	–	–	+	+	Non-GCB	ND	–	ND	
3													
DLBCL, centroblastic	+	– (0)	ND	–	–	–	–	+	Non-GCB	–	ND	ND	Related
DLBCL, centroblastic	+	+ (90)	+	–	–	–	–	+	Non-GCB	–	–	ND	
4													
DLBCL, centroblastic	+	– (0)	–	–	–	–	+	+	Non-GCB	–	ND	ND	ND
DLBCL, centroblastic	+	+ (60)	ND	–	–	–	+	+	Non-GCB	–	–	ND	
5													
DLBCL, centroblastic	+	ND	ND	ND	ND	ND	ND	ND	ND	ND	ND	ND	
DLBCL, centroblastic	+	– (0)	ND	–	–	–	+	+	Non-GCB	ND	ND	ND	Related
DLBCL, centroblastic	+	+ (80)	ND	–	–	–	+	+	Non-GCB	–	–	ND	
6													
FL, grade 2	+	– (0)	ND	–	+	–	ND	ND	GCB	ND	ND	IGH/BCL2 fusion +	ND
DLBCL, centroblastic	+	+ (100)	ND	–	–	–	ND	ND	ND	ND	ND	IGH/BCL2 fusion +	
7													
MALT lymphoma	+	– (0)	ND	ND	–	–	ND	ND	ND	–	ND	ND	ND
DLBCL, centroblastic	+	+ (80)	ND	–	–	–	ND	ND	ND	ND	ND	ND	
8													
LPL/BM	+	– (0)	–	–	–	–	–	+	Non-GCB	–	ND	ND	Related
DLBCL, centroblastic	+	+ (90)	ND	–	–	–	ND	ND	ND	–	ND	ND	
9													
DLBCL, centroblastic and FL, grade 3b	+	+‡ (100)	ND	–	+‡	+‡	+‡	+‡	GCB	ND	ND	IGH/BCL2 fusion –	

DLBCL, diffuse large B-cell lymphoma; EBER-1 ISH, Epstein-Barr virus–encoding RNA-1 in situ hybridization; FISH, interface fluorescence in situ hybridization; FL, follicular lymphoma; GCB, germinal center B-cell phenotype; LPL, lymphoplasmacytic lymphoma; MALT, mucosa-associated lymphoid tissue; ND, not done.
* By immunohistochemical analysis. Numbers in parentheses are the percentage of positive cells.
† By flow cytometry.
‡ Positive in the DLBCL and FL, grade 3b components.

DOI: 10.1309/AJCP58FETFGLCKKW

only in case 9, composite CD5+ DLBCL and FL grade 3b. Bcl-6 and MUM1 were positive in 5 of 6 CD5+ DLBCLs, and 2 were classified as the GCB phenotype and 4 as the non-GCB phenotype. p53 expression was less than 10% in all 5 cases tested. EBER-1 ISH was negative in all 5 cases tested. In all specimens (CD5– DLBCL, CD5– low-grade B-cell lymphoma, and CD5+ DLBCL) from 9 cases of secondary CD5+ DLBCL, CD5 was restained in parallel by the avidin-biotin complex method, and reproducibility of the CD5 expression (positive or negative result) was confirmed in all of them.

Paraffin-embedded tissue sections of CD5– and CD5+ tumors were available in 6 cases, and a total of 12 samples was applied to molecular analysis. Monoclonal rearrangements of the *CDR3* gene were detectable in 10 samples (83%), and sets of CD5– and CD5+ tumors were available for sequencing in 4 cases. The 2 tumors were clonally related in the 4 cases (Table 2).

Immunohistochemical Studies for CD5 Expression in 30 Patients With DLBCL Undergoing Sequential Biopsies

Transition of CD5 expression was examined by immunohistochemical analysis in 30 patients who underwent sequential biopsies among a total of 529 patients with DLBCL ▮Table 3▮. The number of sequential biopsies was 2 in 26 cases, 3 in 3 cases, and 5 in 1 case. The transition of CD5

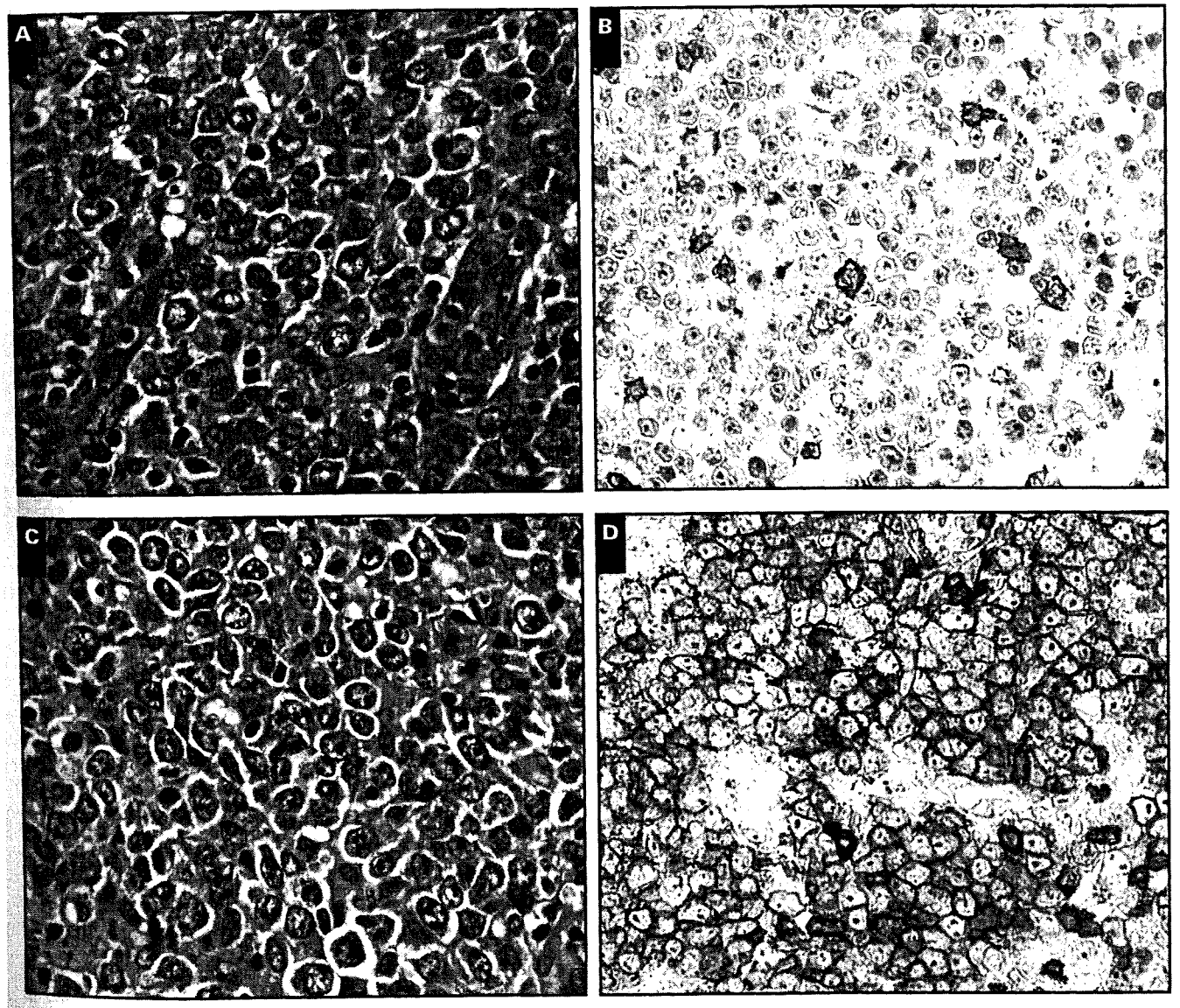

▮Image 1▮ (Case 4) Secondary CD5+ diffuse large B-cell lymphoma (DLBCL) derived from CD5– DLBCL. **A** and **B**, CD5– DLBCL in lymph node at initial diagnosis (**A**, H&E, ×400; **B**, CD5 by immunohistochemical analysis, ×400). **C** and **D**, CD5+ DLBCL in lymph node at relapse (**C**, H&E, ×400; **D**, CD5 by immunohistochemical analysis, ×400).

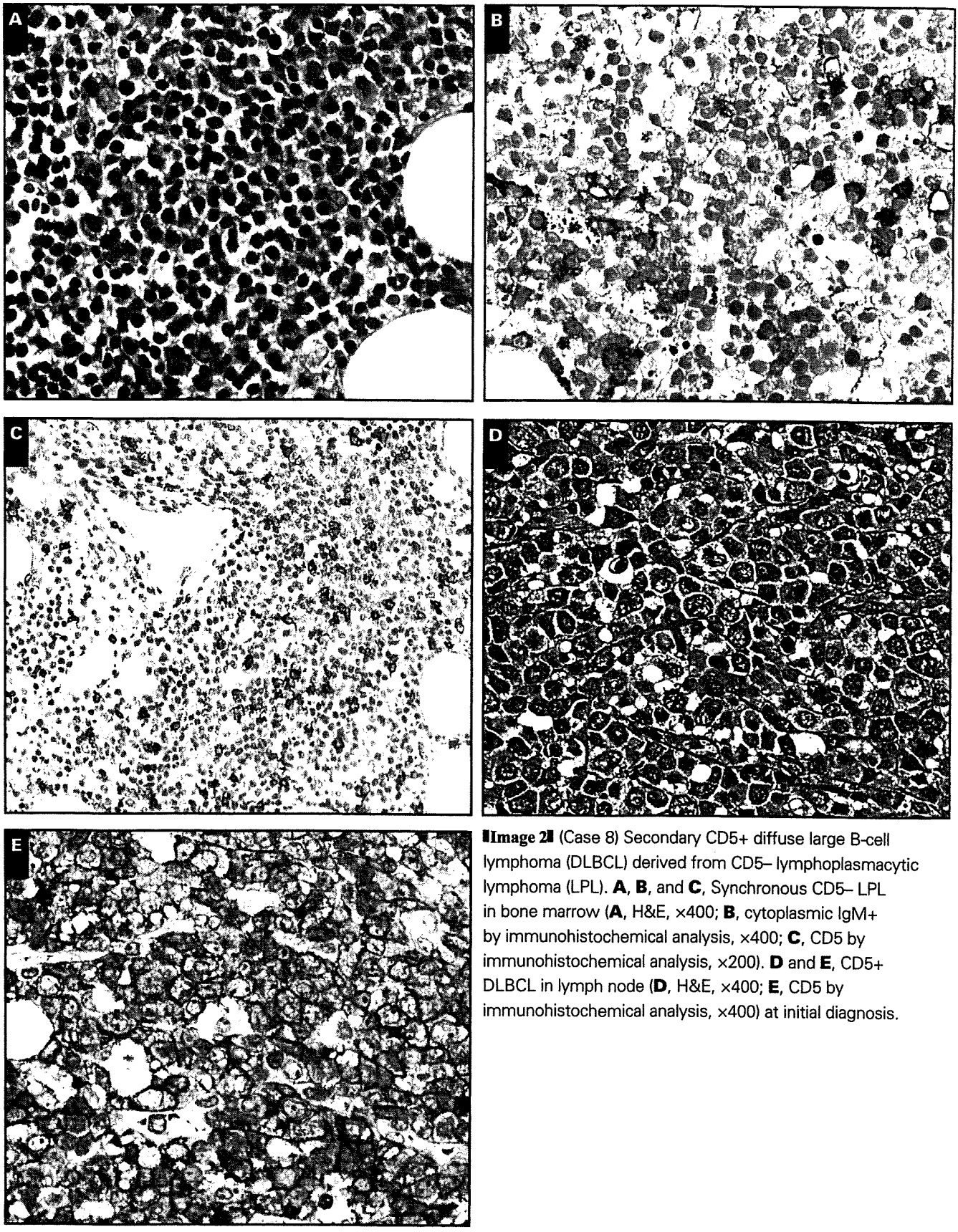

Image 2 (Case 8) Secondary CD5+ diffuse large B-cell lymphoma (DLBCL) derived from CD5– lymphoplasmacytic lymphoma (LPL). **A**, **B**, and **C**, Synchronous CD5– LPL in bone marrow (**A**, H&E, ×400; **B**, cytoplasmic IgM+ by immunohistochemical analysis, ×400; **C**, CD5 by immunohistochemical analysis, ×200). **D** and **E**, CD5+ DLBCL in lymph node (**D**, H&E, ×400; **E**, CD5 by immunohistochemical analysis, ×400) at initial diagnosis.

DOI: 10.1309/AJCP58FETFGLCKKW

expression was –/– in 20 cases, –/–/– in 2 cases, –/–/–/–/– in 1 case, –/+ in 4 cases, –/+/+ in 1 case, and +/+ in 2 cases; no case showed +/–.

Reproducibility of Data From Flow Cytometry and Immunohistochemical Studies in 89 DLBCLs

Among a total of 728 DLBCLs, flow cytometry results were available for 89 cases, and, therefore, the CD5 expression data obtained by immunohistochemical analysis and flow cytometry were compared. These results corresponded in 99% of the cases (88/89), including 83 cases with a CD5– phenotype and 5 cases with a CD5+ phenotype. The remaining case was CD5+ by immunohistochemical analysis and CD5– by flow cytometry.

Table 3
Transition of CD5 Expression in 529 Cases of DLBCL as Shown by Immunohistochemical Analysis*

Biopsy					
First	Second	Third	Fourth	Fifth	No. of Cases
–					464
–	–				20
–	–	–			2
–	–	–	–	–	1
–	+				4
–	+	+			1
+					35
+	+				2

DLBCL, diffuse large B-cell lymphoma.
* In 499 cases, 1 biopsy was done; in 30 cases, 2 or more biopsies were done.

Discussion

Among a total of 529 patients with DLBCL, 38 (7.2%) had CD5+ DLBCL. Probably because sequential biopsies were not infrequently performed at our institution, 9 cases (9/38 [24%]) of secondary CD5+ DLBCL were identified. All of them were non–Richter syndrome secondary CD5+ DLBCL. One of the most likely reasons for the lack of Richter syndrome cases in our series is that the frequency of CLL/SLL is very low in Japan compared with Western countries (1.3%).[20]

The 9 cases of non–Richter syndrome secondary CD5+ DLBCL were classifiable into 3 groups. Five cases constituting group 1 gained CD5 during the clinical course of DLBCL, and corresponded to 18% of patients (5/28) with DLBCL in whom sequential biopsies showed CD5– at the first biopsy. Thus, if rebiopsies are performed more frequently at relapse, more secondary CD5+ DLBCLs might be detected. The 3 cases constituting group 2 gained CD5 at the time of transformation from CD5– low-grade B-cell lymphoma. Except for our 1 reported case,[17] there has been no previous example of CD5– low-grade B-cell lymphoma transforming to CD5+ DLBCL. The sole case in group 3 showed a shift of CD5+ FL grade 3b to CD5+ DLBCL. Recently, it has been reported that CD5+ FL can transform to DLBCL.[13,14]

In the present study, we were unable to conclude that patients with non–Richter syndrome secondary CD5+ DLBCL had a poor outcome because the number of cases was small. However, group 1 and 2 tumors gained CD5 during the clinical course of CD5– DLBCL or transformation of CD5– low-grade B-cell lymphoma. Moreover, in 30 cases of DLBCL in which the patients underwent sequential biopsies, 5 showed a change of CD5 expression from negative to positive, but none changed from positive to negative. It was suggested that CD5 could be gained in association with tumor progression in DLBCL. This is in contrast with the fact that the B-chronic lymphocytic leukemia–specific markers CD5 and CD23 are frequently lost during transformation to DLBCL (Richter syndrome).[21] If some cases of non–Richter-syndrome secondary CD5+ DLBCL in group 1 or 2 had been included in previously reported de novo CD5+ DLBCL, it would have been consistent with the role of CD5 as a progression marker in de novo CD5+ DLBCL.

The frequency of CD5+ DLBCLs among the total DLBCLs in the present series was 7.2%, which was lower than the figure of 10% reported by Yamaguchi et al.[5] However, they performed immunohistochemical analysis on frozen tissue sections, whereas we used paraffin-embedded tissue sections, which could have led to false negativity. However, the high reproducibility of CD5 expression between flow cytometry and immunohistochemical analysis and between the polymer method and the avidin-biotin complex method of immunohistochemical analysis indicated that the CD5 expression data obtained by immunohistochemical analysis on paraffin-embedded tissues were not inferior to those obtained by flow cytometry. Therefore, we considered that the incidence of false negativity for detection of CD5 expression by immunohistochemical analysis on paraffin-embedded tissues was very low in DLBCLs.

Secondary CD5+ DLBCL was found to account for 24% of CD5+ DLBCL cases (9/38). Three groups of non–Richter syndrome secondary CD5+ DLBCL were identified and were shown to be derived from CD5– DLBCL, CD5– low-grade B-cell lymphoma, and CD5+ FL. In groups 1 and 2, CD5 was gained during the clinical course or transformation of tumors, suggesting that CD5 expression is closely associated with the progression of B-cell lymphoma.

From the [1]Clinical Laboratory and [2]Hematology and Stem Cell Transplantation Divisions, National Cancer Center Hospital, Tokyo, Japan; and [3]Department of Surgical Pathology, Hokkaido University Hospital, Sapporo, Japan.

Address reprint requests to Dr Maeshima: Clinical Laboratory Division, National Cancer Center Hospital, Tsukiji 5-1-1, Chuo-ku, Tokyo 104-0045, Japan.

Acknowledgments: We thank C. Kina and S. Miura for technical assistance with the immunohistochemical studies.

References

1. Harris NL, Ferry JA. Follicular lymphoma. In: Knowles DM, ed. *Neoplastic Hematopathology*. 2nd ed. Philadelphia, PA: Lippincott Williams & Wilkins; 2001:823-853.
2. Kipps TJ. The CD5 B cell. *Adv Immunol*. 1989;47:117-185.
3. Matolcsy A, Chadburn A, Knowles DM. De novo CD5-positive and Richter's syndrome-associated diffuse large B cell lymphomas are genotypically distinct. *Am J Pathol*. 1995;147:207-216.
4. Kroft SH, Howard MA, Picker LJ, et al. De novo CD5+ diffuse large B-cell lymphomas: a heterogeneous group containing an unusual form of splenic lymphoma. *Am J Clin Pathol*. 2000;114:523-533.
5. Yamaguchi M, Seto M, Okamoto M, et al. De novo CD5+ diffuse large B-cell lymphoma: a clinicopathologic study of 109 patients. *Blood*. 2002;99:815-821.
6. Murase T, Yamaguchi M, Suzuki R, et al. Intravascular large B-cell lymphoma (IVLBCL): a clinicopathologic study of 96 cases with special reference to the immunophenotypic heterogeneity of CD5. *Blood*. 2007;109:478-485.
7. Ferry JA, Yang WI, Zukerberg LR, et al. CD5+ extranodal marginal zone B-cell (MALT) lymphoma: a low grade neoplasm with a propensity for bone marrow involvement and relapse. *Am J Clin Pathol*. 1996;105:31-37.
8. Ballesteros E, Osbome BM, Matsushima AY. CD5+ low-grade marginal zone B-cell lymphomas with localized presentation. *Am J Surg Pathol* 1998;22:201-207.
9. Lin CW, O'Brien S, Faber J, et al. De novo CD5+ Burkitt lymphoma/leukemia. *Am J Clin Pathol*. 1999;112:828-835.
10. Tiesinga JJ, Wu CD, Inghirami G. CD5+ follicle center lymphoma: immunophenotyping detects a unique subset of "floral" follicular lymphoma. *Am J Clin Pathol*. 2000;114:912-921.
11. Barekman CL, Aguilera NA, Abbondanzo SL. Low-grade B-cell lymphoma with coexpression of both CD5 and CD10: a report of 3 cases. *Arch Pathol Lab Med*. 2001;125:951-953.
12. Barry TS, Jaffe ES, Kingma DW, et al. CD5+ follicular lymphoma: a clinicopathologic study of three cases. *Am J Clin Pathol*. 2002;118:1051-1057.
13. Catherwood MA, Venkatraman L. Follicular origin of a subset of CD5+ diffuse large B-cell lymphomas [letter]. *Am J Clin Pathol*. 2006;125:954-955.
14. Vasallo J, Bousquet M, Quelen C, et al. CD5-positive diffuse large B-cell lymphoma arising from a CD5-positive follicular lymphoma. *J Clin Pathol*. 2007;60:573-575.
15. Miyawaki S, Machii T, Hirabayashi H, et al. Splenic lymphoma with callous lymphocytes with CD5+, CD11c+ B-cell phenotype. *Intern Med*. 1993;32:472-475.
16. Fujisawa S, Tanioka F, Matsuoka T, et al. CD5+ diffuse large B-cell lymphoma with *c-myc/IgH* rearrangement presenting as primary effusion lymphoma. *Int J Hematol*. 2005;81:315-318.
17. Maeshima AM, Omatsu M, Nomoto J, et al. Diffuse large B-cell lymphoma after transformation from low-grade follicular lymphoma: morphological, immunohistochemical and FISH analyses. *Cancer Sci*. 2008;99:1760-1768.
18. Hans SP, Weisenburger DD, Greiner TC, et al. Conformation of molecular classification of diffuse large B-cell lymphoma by immunohistochemistry using a tissue microarray. *Blood*. 2004;103:275-282.
19. Sekiguchi N, Kobayashi Y, Yokota Y, et al. Follicular lymphoma subgrouping by fluorescence in situ hybridization analysis. *Cancer Sci*. 2005;96:77-82.
20. Lymphoma Study Group of Japanese Pathologists. The World Health Organization classification of malignant lymphomas in Japan: incidence of recently recognized entities. *Pathol Int*. 2000;50:696-702.
21. Mao Z, Quintanilla-Martinez L, Raffeld M, et al. IgV_H mutational status and clonality analysis of Richter's transformation. *Am J Surg Pathol*. 2007;31:1605-1614.

DOI: 10.1309/AJCP58FETFGLCKKW

Abdominal Imaging

Abdom Imaging (2009)
DOI: 10.1007/s00261-009-9516-9

Nodal status of malignant lymphoma in pelvic and retroperitoneal lymphatic pathways: PET/CT

Ukihide Tateishi,[1] Takashi Terauchi,[2] Tomio Inoue,[1] Kensei Tobinai[3]

[1]Department of Radiology, Yokohama City University Graduate School of Medicine, 3-9, Fukuura, Kanazawa-ku, Yokohama, Kanagawa 236-0004, Japan
[2]Division of Cancer Screening, Research Center for Cancer Prevention and Screening, National Cancer Center, Tokyo, Japan
[3]Hematology and Stem Cell Transplantation Division, National Cancer Center Hospital, Tokyo, Japan

Abstract

Nodal involvement of abdominal lymphatic pathways occurs in a number of histologic subtypes of malignant lymphoma. The histologic diagnosis of abnormal uptake in abdominal lymphatic pathways includes mainly non-Hodgkin lymphoma with B-cell lineage and Hodgkin lymphoma. Initial involvement of pelvic and retroperitoneal lymphatic pathways can result from a variety of underlying non-Hodgkin's lymphoma: follicular lymphoma, diffuse large B-cell lymphoma, marginal zone B-cell lymphoma of mucosa-associated lymphoid tissue (MALT) type, and mantle cell lymphoma. The diagnosis of these clinical entities requires various imaging techniques, including fluorine-18-fluorodeoxyglucose (^{18}FDG) positron emission tomography/computed tomography (PET/CT), computed tomography, ^{67}Gallium scintigraphy, and magnetic resonance imaging (MRI). Specific symptoms of these diseases are often lacking, but intense ^{18}FDG accumulation on PET/CT may be a marker of disease activity. Interpretation of the presence of and the specific pattern of ^{18}FDG uptake may obviate the need for invasive biopsy. However, distinction of abnormal uptake is often difficult to determine because focal accumulation of ^{18}FDG in the urinary tract or intestine mimics nodal involvement in the pelvic and retroperitoneal lymphatic pathways. In this review, specific conditions causing nodal involvement of pelvic and retroperitoneal lymphatic pathways in patients with malignant lymphoma that may impact diagnostic and treatment decisions are highlighted.

Correspondence to: Ukihide Tateishi; *email:* utateish@yokohama-cu.ac.jp

Published online: 16 April 2009

Key words: PET—PET/CT—Malignant lymphoma

Malignant lymphoma most often involves lymph nodes of pelvic and retroperitoneal lymphatic pathways at the initial staging. Nodal involvement within the pelvic or retroperitoneal lymphatic pathways results from disparate disease status. Tumor stage in malignant lymphoma is assessed initially by conventional imaging modalities such as positron emission tomography/computed tomography (PET/CT), PET, computed tomography (CT), magnetic resonance imaging (MRI), and ^{67}Gallium scintigraphy, which can play an important role in the initial determination of the stage because they provide morphologic information on the extent of disease. Fluorine-18 fluorodeoxyglucose (^{18}FDG) PET/CT or PET is a valuable tool for staging of patients with malignant lymphoma [1–3], therapeutic effect [4–7], and prediction of prognosis [8] in most histologic subtypes [9–13]. The anatomic location and specific features of ^{18}FDG accumulation often provide insights into disease activity and can sometimes explain occult disease progression. However, evaluation of pelvic or retroperitoneal nodal status with PET/CT can be complicated by urinary and intestinal activity or anatomic variants [14–16]. Discrete comparison with diagnostic contrast-enhanced CT study when evaluating PET/CT is often disturbed by misregistration, but contrast-enhanced PET/CT can improve anatomical localization of pelvic and retroperitoneal lesions. This review organizes the classification of malignant lymphomas involving pelvic and retroperitoneal lymph node, outlines anatomic distribution of pelvic and retroperitoneal lymph nodes, illustrates their PET/CT features, and summarizes method of detection.